April 2016

Ethanol Dehydration with ZSM-5

Alexander Joseph Zitoli
Worcester Polytechnic Institute

Jennifer Ann Coffey
Worcester Polytechnic Institute

Ethanol Dehydration with Zeolite ZSM-5

A Major Qualifying Project Report

Submitted to the Faculty of the

WORCESTER POLYTECHNIC INSTITUTE

In partial fulfillment of the requirements for the

Degree of Bachelor of Science

In Chemical Engineering

By

_____

Jennifer Coffey

_____

Alexander Zitoli

April 28, 2016

Approved:

_____

Professor Michael Timko, Advisor

Abstract

In the global effort to reduce fossil fuel reliance, green ethylene is being produced through vapor phase catalytic dehydration of bio-ethanol. This project studied the benefits of ethanol dehydration with zeolite ZSM-5 in the liquid phase. Process variables manipulated were phase, feed flowrate ratio, and volume-hourly space velocity. Through gas chromatography, it was determined that liquid phase dehydration had comparable ethanol conversion and superior ethylene production on a per gram of catalyst basis. Further investigation of process variables is recommended.

Table of Contents

List of Figures

Chapter 1: Introduction

Ethylene is a commodity product that is used daily by millions of people. From plastic water bottles to adhesives, ethylene plays a large role in modern day life. The global demand for ethylene is greater than 156 million tons annually (Fan et. al, 2013). Currently, the vast majority of ethylene is produced from fossil fuels. Ethylene production from ethanol has gained growing interest as an environmental alternative to fossil fuels. Producing bio-ethanol from corn and sugarcane in the United States and Brazil, respectively, has been successful in recent years. Traditionally, ethylene has been produced by cracking fossil fuels. However, to make this process competitive compared to current oil refineries, considerable improvements must be made. Economic benefits would help drive a method of bio-ethylene production can be developed that is an attractive green alternative. Figure 1 shows a sequence of processing could provide green commodity products.

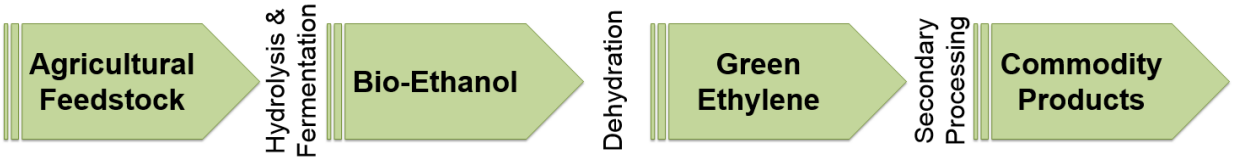

Figure 1: Route to Green Commodity Products

Bio-ethanol would continue to be produced from the fermentation of agricultural byproducts such as sugar cane or corn stover. It would then undergo catalytic dehydration to produce green ethylene, which is a drop in replacement for petro-produced ethylene.

While bio-ethylene production has undeniable environmental benefits- there are many factors preventing it from growing to be the main source of ethylene and its derivatives. Bio-based plastic production produces 327,000 tons a year compared to 12.3 million tons a year of plastics made from petrochemicals (Williams, 2010). Opposition in America to bio-based products is often centered on the argument regarding direct and indirect impacts on food production. The concern is that land will be unequally distributed between commodity production and food production. Many of the crops that bio-based plastics come from are also very resource intensive. For example, corn nearly depletes the land it is grown on of all nutrients, requiring future crops to rely heavily on fertilizers- which have their own set of well

documented, negative effects on the environment. Additionally, industry has not latched onto bio-based plastics because of the added cost. That cost is eventually passed on to the customer. The most notable company using bio-ethylene is Coca-Cola with their "Plant Bottle." Currently Coca-Cola is absorbing the cost of using bio-ethylene while further research and development aims to lower costs. They have pledged that all Coca-Cola Brand bottles will be 30% plant based by 2020 (Plant Bottle FAQ, 2015).

Large feed stocks of sugar cane and corn enable industrial scale production of bio-ethylene. Bio-ethylene is identical in chemical structure and reactivity to petrochemical ethylene. This makes it a drop-in substitute, meaning companies do not need to alter their current processes or equipment before they begin to use bio-ethylene. Production and use of bio-ethylene generates 10% of the green-house gases associated with petro-based ethylene (Brazilian Sugarcane Industry Association, 2015). Eliminating the need for ethylene generated from fossil fuels with bio-ethylene is not feasible at this point in time. One company that has had particular success with bio-ethylene production is Braskem, located in Brazil. Historically, Braskem is known best as a petrochemical company holding group. Ironically, they are now the most notable bioplastic producer in the entire world. A major source of their success is smart supply chain usage (Luiz et. al, 2013). Their plants are located near where the bio-ethanol is produced, as Brazil produces 588 million tons of sugarcane each year. A substantial amount of Brazil's sugar cane is fermented into bio-ethanol. Braskem has produces bio-ethanol from sugar cane without effecting the countries food supply or the rain forest

Industry currently uses a series of fixed bed, adiabatic reactors to carry out the dehydration of bio-ethanol. Ethanol dehydration is a zero-order endothermic reaction that favors the production of ethanol. High temperature and pressure drives the equilibrium in favor of the production of ethylene (Cameron, Levine & Nagulapalli, 2012). Fixed bed reactors inherently require a catalyst to work over a large temperature range. Unfortunately, catalysts with the highest selectivity for ethylene production have very high and small ideal temperature ranges. Additionally, the products of vapor phase ethanol dehydration are also difficult to separate. Many products similar to ethylene are produced requiring several separation steps to isolate ethylene.

A method that has been under particularly rigorous study is the use of a zeolite catalyst. At Worcester Polytechnic Institute (WPI), ethanol dehydration is being investigated with the use of the zeolite catalyst, ZSM-5. In the reaction mechanism, ZSM-5 acts as a bronsted acid site that facilitates dehydration. However, numerous studies have indicated that the concentration of active acid sites on ZSM-5 decreases significantly over time when reactions are run continuously. Additionally, fouling of the catalyst occurs when species within the reaction deposit on the surface of the catalyst, blocking sites of activity (Zhang et. al, 2008).

The main goal of this project was to optimize the liquid phase zeolite catalyzed dehydration of ethanol to contribute to the current industrial processes used to create ethylene from bio-ethanol. Data were collected over the course of seven months by two undergraduate students with the help of a PhD candidate. From the results of this project, recommendations were developed on how to improve the current ethanol dehydration process being investigated at WPI. This project aims to provide evidence of a liquid phase advantage. Additionally, this project aimed to contribute to a growing body of research on liquid phase chemical processes for bio-refineries.

Data was collected over 41 experimental trials that lasted between four and eight hours depending on the activity of the reaction. Trials were run in both the liquid and vapor phase. Experiments were conducted using a ZSM-5 packed bed micro-reactor. The volume-hourly space velocity (VHSV) was the variable manipulated in order to compare the efficacy of the liquid phase reactions. Ethanol and water were co-fed to the reactor at a ratio of 2:1 volume percent. Upon exiting the micro-reactor, the gas and liquid phase products were sent to a glass column for collection. The gas products were fed to the gas chromatograph (GC) for further analysis. Liquid products were collected periodically and analyzed in batches. From the GC, the continuously generated graph of intensity vs. retention time was used to identify and quantify each product species. The intensity of generated peaks was further analyzed with calibration curves to determine conversion and yield. The amounts of each species were calculated by integrating the areas of the peaks that corresponded to each species.

Initial trials were used to determine the optimal feed ratio of 2:1 (ethanol: water). Different temperatures were investigated. Liquid phase reactions ensure better heat exchange throughout the reaction media. When comparing liquid and gas phase interactions, the liquid

phase has more contact between molecules and surface area for heat transfer. The stability of the catalyst and the optimization of the temperature regime are barriers in the optimization of this chemical process.

Currently, there are three main concerns with the process that are potentially leading to the deactivation of the catalyst: ion exchange, coking, and the framework stability of the temperature regime. Ion exchange, also referred to as leaching, is the phenomena of chemical species of the zeolite dissociating from the primary body of the catalyst into the reaction medium, rendering catalytic sites obsolete. Coking stability, as mentioned earlier, cannot be directly prevented or reversed when using powdered ZSM-5. Leaching and coking stability cannot be quantified sufficiently with the lab equipment available. However, the effects of the temperature regime can be directly observed based on the ethanol conversion and ethylene yield at different temperatures within the range of 250-450°C.

In early trials, the liquid and vapor phase were compared by operating at the same weight-hourly space velocities (WHSV's). However, to account for differences in the density of the liquid and vapor phases, the VHSV was chosen as a comparison variable instead of the WHSV. Comparison of the VHSV's showed that at the same space velocities, liquid phase dehydration has a higher ethylene yield and lower ethanol conversion than the vapor phase. In contrast, the vapor phase has a higher ethanol conversion than the liquid phase, but the liquid phase trials demonstrated greater throughput than the vapor phase.

Chapter 2: Background

This project studies the benefits of performing ethanol dehydration with ZSM-5 in the liquid phase versus the vapor phase. This chapter provides background information on the industry that does ethanol dehydration with zeolites, catalysis and ZSM-5, the mechanism of ethanol dehydration, vapor and liquid phase dehydration, and elements of reactor design. Although vapor phase dehydration and zeolites are well researched in the bio-ethylene industry, this project explores the potential for liquid phase dehydration to generate a higher product purity and greater throughput than vapor phase dehydration. In addition to providing background information on current industrial practices and the dehydration mechanism, this chapter will investigate the criteria that determine the efficiency of a process.

2.1 Bio-Ethylene Industry

Ethylene is a commodity product that is used daily by millions of people, resulting in a global demand for ethylene greater than 156 million tons annually (Fan, 2013). Traditionally, ethylene is produced from petroleum, but ethylene production from ethanol has gained a growing environmental and financial interest (Haro et. al, 2013). Conventionally, ethylene has been produced by cracking fossil fuels, but ethylene production from bio-ethanol from corn and sugarcane in the United States and Brazil, respectively, has been successful in recent years.

Large feed stocks of sugar cane and corn enable industrial scale production of bio-ethylene. Bio-ethylene is identical in chemical structure and reactivity to petrochemical ethylene. This makes it a drop-in substitute, meaning companies do not need to alter their current processes or equipment before they begin to use bio-ethylene. Production and use of bio-ethylene generates 10% of the green-house gases associated with petro-based ethylene (Brazilian Sugarcane Industry Association, 2015). Eliminating the need for ethylene generated from fossil fuels with bio-ethylene is not feasible at this point in time. One company that has had particular success with bio-ethylene production is Brazil's Braskem. Historically, Braskem is known best as a petrochemical company holding group. Ironically, they are now the most notable bioplastic producer in the entire world. A major source of their success is smart supply chain usage (Luiz, 2013). Their plants are located near where the bio-ethanol is produced, as Brazil produces 588 million tons of sugarcane each year. A substantial amount of Brazil's sugar cane is fermented into bio-ethanol via catalytic dehydration.

2.2 Catalysis

Catalysis, the study of catalysts, supports many industries around the world such as petroleum refining, the food industry, energy generation, and the chemical industry. Estimates from the North American Catalysis Society state that catalysis contributes to more than 35% of the global gross domestic product (GDP), making the study of catalysts and catalyst-aided reactions extremely valuable and relevant to the global economy. Particularly, the chemical industry relies heavily on catalysts to decrease production costs and increase efficiency (What is Catalysis?, 2008).

2.3 Zeolites

Zeolites are a group of natural and synthetic hydrated aluminum silicates (Sadaba, 2015). Zeolites possess a three-dimensional framework formed by silica and alumina tetrahedrons. Oxygen atoms organize themselves around the silica and alumina atoms and ions, respectively. An image of these tetrahedrons is shown below.

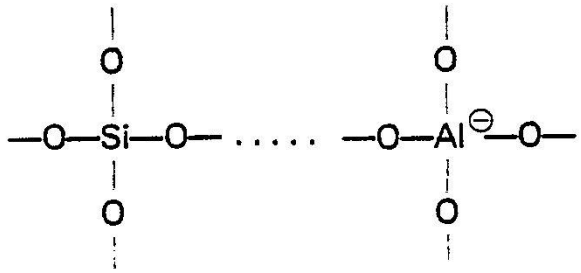

Figure 2: Structural Formula Depicting Aluminasilicate Attractions in Zeolite Structures

The negative charge on the alumina tetrahedron and the nucleophilic properties of the silica tetrahedron form the active sites of the zeolite. The tetrahedrons form a large system of cavity-like active sites that attract positive ions and organic molecules that are small enough to fit into the cavities. As catalysts, these cavities help decrease the activation energy of reactions by providing an active site for the reaction to initiate (Zeolites, 2016).

2.3.1 Zeolites in Industry

Zeolites are valuable as catalysts because of their relative low cost and high concentration of active Bronsted acid sites. Additionally, natural and synthetic zeolites are easier to obtain and

process than higher value transition metal catalysts. The well-defined and consistent structure of zeolites allows for relatively consistent results in industrial processes. However, zeolites are susceptible to degradation via coking, leaching, and breakdown of the framework. The solvents, reactants, temperature, and reaction conditions used in the presence of zeolites can lead to degeneration (Sadaba, 2015).

2.4 Ethanol Dehydration Mechanism

Ethanol dehydration is a zero-order endothermic reaction that favors the production of ethanol. High temperature and pressure drives the equilibrium in favor of the production of ethylene (Cameron, 2012). Fixed bed reactors inherently require a catalyst to work over a large temperature range. Unfortunately, catalysts with the highest selectivity for ethylene production have very high and small ideal temperature ranges. Problems encountered in the dehydration of ethanol can be explained by a triangular network of reactions proposed by Luiz et. al, shown in Figure 3, which produce undesired products that inhibit ethylene production and add separation costs.

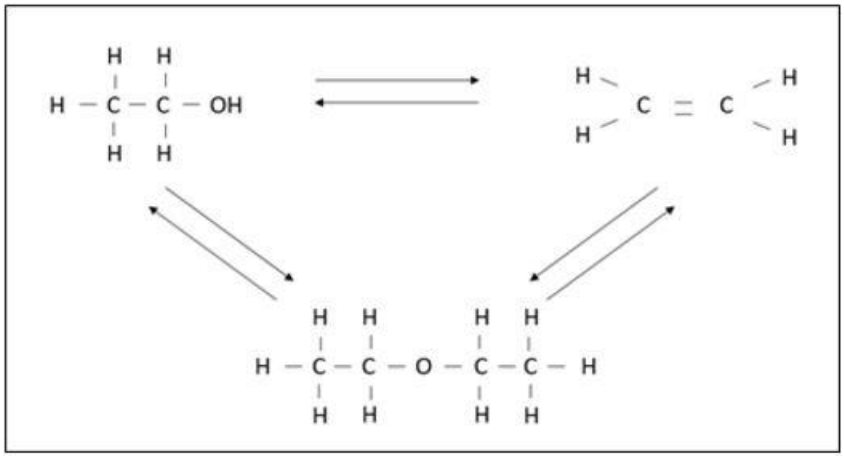

Figure 3: Possible Ethanol Dehydration Triangular Reaction Network based on Luiz

There are many reaction methods being studied currently, the main question with this triangular network is if the reaction between diethyl ether and ethylene is reversible. More study of the mechanism is need to understand how to minimize by-products and increase ethylene yield at lower temperatures. Operation in the sub-critical range is necessary in order for industry to fully adopt bio-ethylene.

A large body of research has contributed to the feasibility of carrying out catalytic ethanol dehydration in the sub-critical range. In a study by Chen et. al, catalytic ethanol dehydration was tested with SAPO as the catalyst. An investigation of the temperature regime determined that the highest catalytic activity for ethanol and ethylene was in the range of 340-440˚C (Chen et. al, 2010).

2.5 Ethanol Dehydration with ZSM-5

Zeolite Socony Mobil-5 (ZSM-5) is an aluminosilicate zeolite patented by Mobil Oil Company in 1975 (Lisensky, 2010). Research organizations and chemical companies have investigated the physical and chemical properties of ZSM-5 under a variety of conditions to determine the efficacy of ZSM-5 as a catalyst. Particularly, a joint study by the research scientists from the Georgia Institute of Technology, the U.S. Department of Chemistry and Catalysis Research Center, and universities in Germany and Switzerland investigated the stability of ZSM-5 and Zeolite Y with different ratios of Aluminum to Silica in hot liquid water from 150-200˚C. Through a variety of analytical methods like absorption spectroscopy and X-ray diffraction, the group of researchers determined that ZSM-5 did not experience modifications when exposed to hot liquid water under the given conditions (Ravenelle et. al, 2010).

In a study conducted by researchers at the School of Chemical Engineering and Technology at Tianjin University, ZSM-5 and three other catalysts were studied in the catalytic dehydration of ethanol to ethylene. The research group determined that among four catalysts, ZSM-5 exhibited the highest ethanol conversion and the highest selectivity to ethylene, making ZSM-5 a preferred choice for ethanol dehydration (Zhang et. al, 2008). The study also noted that the stability of ZSM-5 had issues with stability over long periods of time due to coking.

A study conducted at the University of Iowa further investigated ethanol dehydration with ZSM-5. Cory Phillips and Ravindra Datta determined that the presence of water in the ethanol feedstock increased catalytic activity and ethylene selectivity. They studied ethanol dehydration in the vapor phase with a feed ratio of 3:1, ethanol to water. The reaction temperature for their investigation was 140-220°C. They purposed that the presence of water was able to prevent coking by tempering the acidity of ZSM-5's active sites (Phillips & Datta, 1997).

2.6 Efficacy Criteria

Multiple criteria are used to analyze collected data for an experiment. Conversion and yield calculations as well as throughput calculations were key evaluative tools for this project. Conversion is defined as the number of moles reacted of a species per mole of the species fed to the reactor (Fogler, 2005). An equation for calculating conversion is show below.

$$Conversion = \frac{Moles\ fed}{Moles\ reacted}$$

Throughput is a criteria used to measure the value and efficiency of an industrial chemical process. Throughput can be measured by the total output of a process or a unit over a specific period of time under normal operating conditions (What is Throughput?, 2016). For analysis, throughput was compared by determining the amount of ethylene generate per gram of catalyst used. When comparing the effects of a variable on a process, changes in throughput are a useful indication of the efficacy of a process.

Chapter 3: Experimental

Ethylene production is young and growing industry where advances in industrial processes could increase efficacy and productivity. Specifically, ethanol dehydration in the liquid phase holds potential for lower energy costs and fits better with the supply chain for the industry. To determine the benefits of liquid phase versus vapor phase ethanol dehydration, the project team accomplished three objectives.

1. To vary the VHSV and feed flow ratios to optimize the production of ethylene.
2. To determine the ethanol conversion and ethylene yield of liquid and vapor phase reactions.
3. To quantify the throughput of ethylene for liquid and vapor phase reaction.

After accomplishing these objectives, the project team was able to analyze the data collected and make recommendation and conclusions on liquid phase and vapor phase ethanol dehydration.

3.1 Safety

Standard safety precautions were taken throughout the entire series of experiments conducted. Personal protective gear was used at all times including safety glasses with side shields and gloves. Gloves were especially important when handling zeolite ZSM-5 as it is a micro-powder that can easily irritate skin. The material safety data sheet for zeolite ZSM-5 can be found in Appendix A. Safety shields were used around the oven during reactions as typical operating temperature was above 300°C and some runs were at pressures as high as 3600 psi. All gas tanks were also secured to a vertical edge using chains to prevent tipping.

3.2 Equipment

The ethanol dehydration reaction in both liquid and vapor phases was carried out in a micro-scale reactor. The reactor was housed in a retrofitted gas chromatograph chamber that allowed for tight temperature control and had ports for inlet and outlets as well as temperature probes. A full schematic can be seen below in Figure 4.

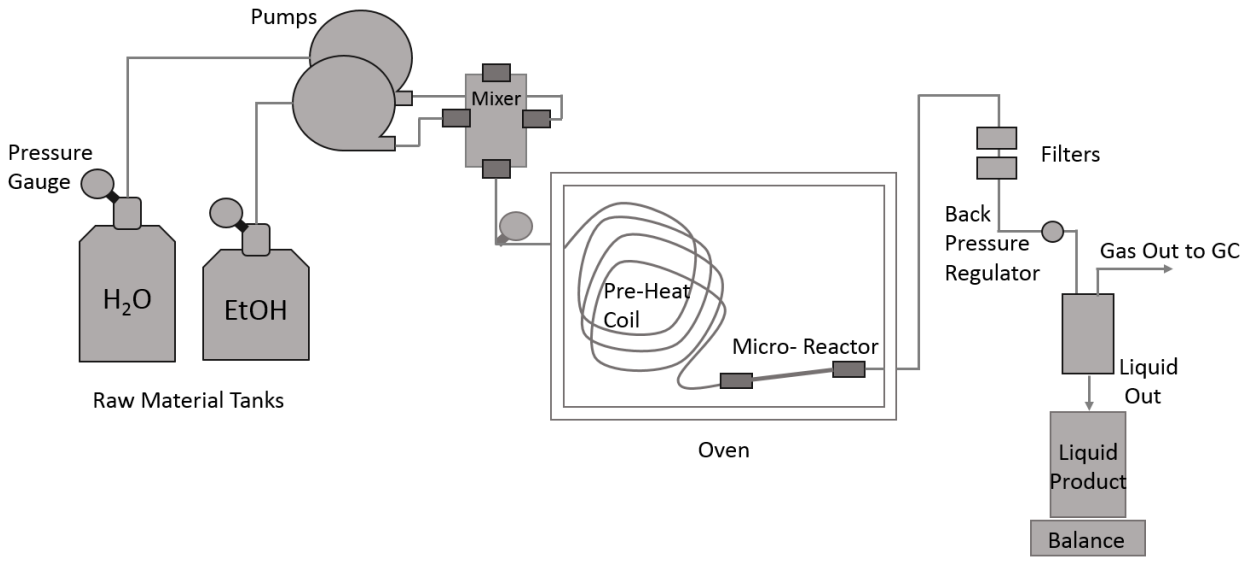

Figure 4: Ethanol Dehydration Equipment Schematic

Reactants are stored within the reactor enclosure and pumped with separate centrifugal pumps. Nitrogen was used as a carrier gas in this study. They pass through a mixing block prior to entering the oven chamber. Upon entering the oven, reactants move through a coil designed to allow them to reach full temperature before entering a packed bed reactor. The outlet end of the reactor is blocked with a porous frit that allowed products to exit but retained the ZSM-5 packed bed. Products flow from the reactor to a glass collection chamber. Liquid products are collected and as gaseous products build pressure they move towards the in-line gas chromatograph. A photograph of the equipment can be seen below in Figure 5:

Figure 5: Picture of Process Unit; Gas Chromatograph not pictured

Throughout this study, the most significant change in the equipment was the length of the outlet piping. The reactor oven was reconfigured to minimize the length of the outlet piping to the gas chromatograph. Operating with the least possible distance to the gas chromatograph provided reliable, reproducible results. Longer outlet pipe lengths lead to pressure build up and sudden release- skewing the results of the in-line gas chromatograph.

3.3 Procedure

A very well defined procedure was followed for each of the 41 experimental trials. The catalyst would be calcined the evening before a trial was scheduled. This process is discussed in detail in section 3.3.1. The reactor was then loaded with the appropriate amount of catalyst and secured in oven of the retrofitted gas chromatograph. The oven was then turned on and allowed to reach temperature. If the trial was to be in the liquid phase, the lines would be pressurized for the pre-heating period to ensure that reactants were in the proper phase from the very beginning of the reaction. Once the oven reached the desired temperature, the pumps and GC-FID were turned on. Gaseous product activity was measured with the GC-FID for the duration of the trial. The glass collection column for liquid products was emptied as needed. Liquid product samples were retained for further analysis. Thorough explanations for each phase of a trial can be found in the following sections.

3.3.1 Catalyst Preparation

ZSM-5 was prepared for each reaction by calcining the desired amount in a crucible for an extended period of time at high temperatures. Calcining ZSM-5 decreases the moisture content of the catalyst, allowing for the reactants to more easily access the active sites within the ZSM-5. The catalyst was initially calcined in a low temperature oven for one hour at 100˚C, and the catalyst was then moved to a 550 ˚C oven for approximately 12 hours. The catalyst was removed from the oven by using long metal tongs to decrease proximity to the heat source, and heat resistant gloves were used to prevent burns and other injuries from occurring in the case of skin contact with the hot crucible. The crucible and catalyst were cooled on a heat resistant brick for 10 minutes, and the desired amount of catalyst was weighed in a weighing tray on a scale that read up to four digits after the decimal place. However, only two digits after the decimal places were used for the actual weight considering the weight of the catalyst did not need to be known after the hundredth decimal place.

3.3.2 Reactor Assembly

Before connecting the reactor to the inlet feed line, a semi-porous metal frit was secured on the outlet of the micro-reactor. The frit required modification in order to fit the reactor outlet. A grinding tool with a fine tip was used in concert with a lathe to rotate and grind the edges of the frit. Once the frit was fitted, the desired amount of catalyst was loaded into the micro-reactor using a small plastic funnel and metal spatula. ZSM-5 is a light, powdery substance, so, when a large amount of catalyst was needed, the catalyst was packed tightly in the reactor using a metal rod. Once the reactor was loaded, the reactor was connected to the inlet and outlet piping of the unit using a wrench. Below is a picture of the two reactors used for the reactions.

Figure 6: Micro reactors Used for Experiment

The smaller top reactor pictured was used for liquid phase runs and the bottom was used for gas phase reactions. Different sized reactors were needed to accommodate different catalyst amounts required to reach desired volume-hourly space velocities.

3.3.3 Reactor Startup

After installing the loaded reactor, the oven door was closed, and the desired temperature was entered as the set point for the oven. Once the desired set point was reached, the nitrogen flow rate was set to approximately 10 ml/min to prevent other gases from entering the feed line. For vapor phase dehydration, the reaction was run at atmospheric pressure without nitrogen pressurization. For liquid phase dehydration, the reaction was run at 3600 psi. The valve on the nitrogen tank was opened and set to 3600 psi to pressurize the system. Following heating of the reactor and pressurization, the ethanol and water feed pumps were set to the desired flow rates.

The pumps were connected to the mixer outside of the reactor which fed into the reactor inlet. Below is a picture of the micro reactor in the oven attached to the inlet and outlet streams.

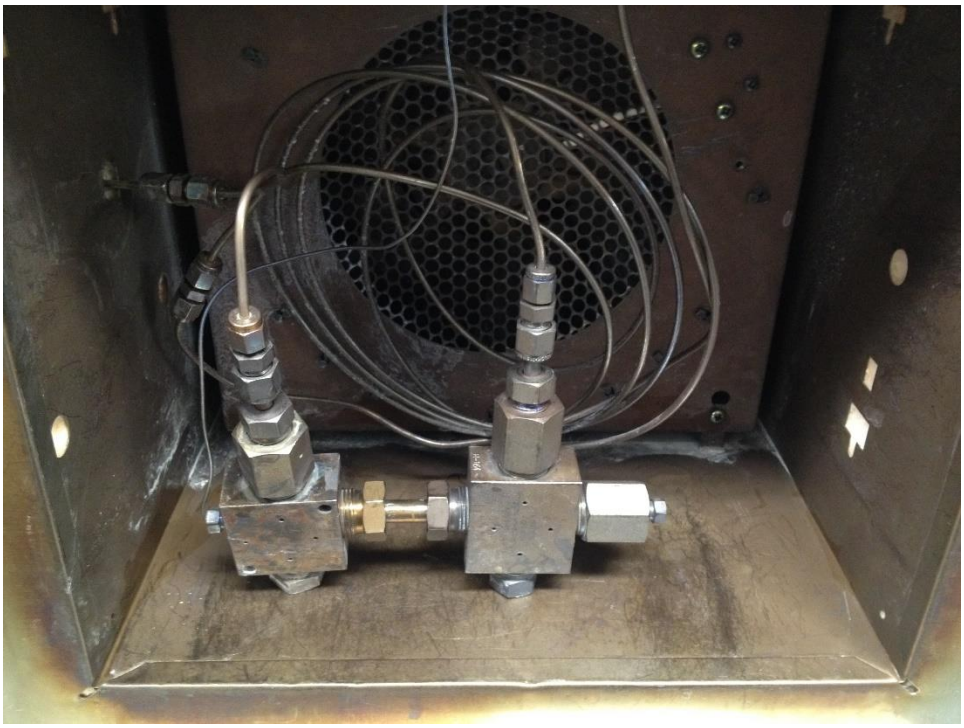

Figure 7: Micro reactor Installed in Oven

Special care was taken to ensure that the reactor was tightly secured to the inlet and outlet blocks. A tight connection was needed to prevent reactants, zeolite and products from being lost when the equipment was pressurized.

3.2 Gas Chromatograph Continuous Gaseous Product Analysis

Immediately after the feed pumps were turned on, the Gas Chromatograph FID (GC-FID) analysis was initiated via a data collection software. To determine the identity and quantity of gaseous species generated by the reaction, a gaseous sample was auto-injected and analyzed every ten minutes from the reactor outlet stream. Figure 8 below shows a picture of the gas chromatograph used.

Figure 8: Gas Chromatograph Equipment Used for Continuous and Batch Analysis

An intensity graph was generated for the gaseous products. Prior to running any experimental trials, a calibration curve was created by injecting sample of known concentrations for analysis with the same method used for in-line analysis. The same gas chromatograph was used for both gaseous and liquid product analysis. Appendix B contains the method files for both the GC-FID and GC-MS analyses.

3.3 Liquid Product Analysis

The reactor outlet was immediately followed by a glass column for product collection. Outlet gas passed through the top of the column to the gas chromatograph while the liquid sample was collected in the column. Glass beads of different diameters were used to reduce the volume of the column to facilitate more consistent production rates. This collection column can be seen below in Figure 9.

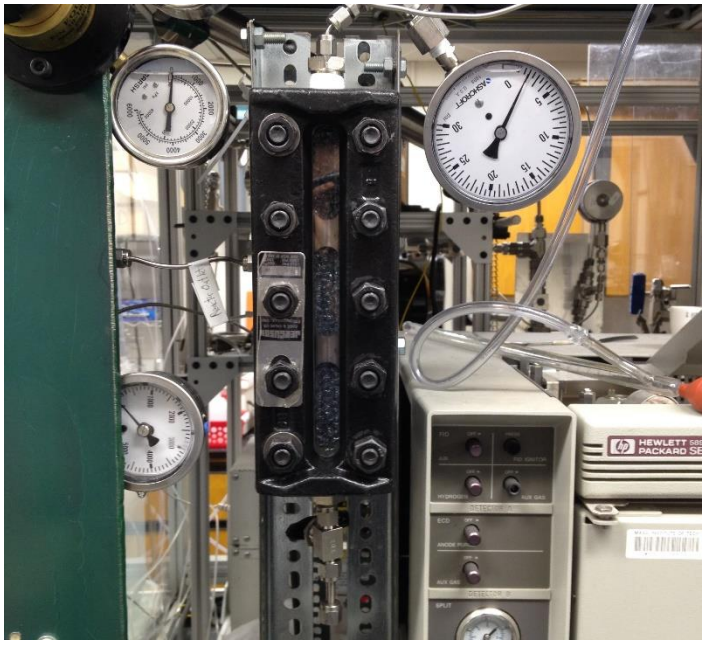

Figure 9: Glass Collection Column for Reactor Outlet

Liquid product samples were collected as the column filled. Special care was taken to ensure that the glass column was not being emptied at the same time a gas sample was being auto-injected to the GC-FID. Collection of liquid samples changed the pressure in the product line which could cause an artificially low activity peak. The sample was collected in a graduated cylinder to determine the volume. The sample was then weighed on a scale to determine the mass. The time over which the sample was generated was recorded and used to determine the mass flow rate and volume flow rate exiting the reactor.

Samples were collected and stored in a freezer until further analysis could be completed. GC-MS was used to identify the components of the liquid product and GC-FID was used to measure the quantity of each product. Samples were diluted for batch analysis. The dilutions used can be seen in Figure 10 below:

Liquid Product Type	Solvent	Sample Amount (µL)	Solvent Amount (mL)
Polar	Water	50	8
Non-Polar	Dodecane	50	8

Figure 10: Liquid Product Dilution Table

Dodecane was used as the carrier solvent for non-polar sample analysis because there was an insignificant amount of dodecane detected in a representative non-polar sample tested with the GC-MS. Toluene was also evaluated as a potential solvent, but interfered with the products of the reaction. When nonpolar samples were analyzed using dodecane, a large presence of toluene was detected.

3.4 Variables Investigated

Throughout this study key variables were varied to determine their effect on ethylene production. High temperature is needed to ensure that this endothermic reaction is thermodynamically favorable. Pressure was used to manipulate the phase of the reaction. At high temperature and pressure, the reaction proceeds in the liquid phase. At high temperatures and atmospheric pressure, the reaction proceeds in the vapor phase. During the first phase of the project, temperature, feed flowrate and feed ratio were constant. This phase involved reactor design and proving that results were reliable and reproducible. In the second phase of the investigation there were slight variations in temperature, catalyst mass and water was introduced to the feed. The third, and most enlightening, phase of the study involved variation of volume-hourly space velocity (VHSV) while catalyst amount, feed ratio and temperature were constant. The following table shows the parameters of the trials involved in the third phase of this study.

Run Number	Phase	Temperature (°C)	Operating Pressure (PSI)	Catalyst Amount (g)	Ethanol Feed Flowrate (mL/min)	Water Feed Flowrate (mL/min)	Feed Ratio	VHSV
22	Vapor	390	14.7	1.6	0.05	0.025	0.66	20.17
23	Liquid	390	3600	0.02	1.5	0.75	0.66	24.35
24	Liquid	390	3600	0.02	0.75	0.375	0.66	12.17
25	Vapor	390	14.7	1.6	0.1	0.05	0.66	40.34
26	Liquid	390	3600	0.02	0.15	0.075	0.66	2.43
27	Vapor	390	14.7	1.6	0.5	0.25	0.66	201.7
28	Liquid	390	3600	0.02	0.3	0.15	0.66	4.87
29	Liquid	390	3600	0.02	1.5	0.75	0.66	24.35
30	Vapor	390	14.7	1.6	0.25	0.125	0.66	100.84
31	Liquid	390	3600	0.02	0.3	0.15	0.66	4.87
32	Liquid	390	3600	0.02	0.5	0.25	0.66	8.12
33	Liquid	390	3600	0.02	0.3	0.15	0.66	4.87
34	Vapor	390	14.7	1.6	0.05	0.025	0.66	20.17
35	Vapor	390	14.7	1.6	0.25	0.125	0.66	100.84
36	Vapor	390	14.7	1.6	0.35	0.18	0.66	141.18
37	Vapor	390	14.7	1.6	0.2	0.1	0.66	80.68
38	Vapor	390	14.7	1.6	0.15	0.77	0.66	60.51
39	Vapor	390	14.7	1.6	0.3	0.154	0.66	121.02
40	Liquid	390	3600	0.01	1.25	0.643	0.66	40.58
41	Liquid	390	3600	0.01	1.85	0.95	0.66	60.07

Figure 11: Trial Parameters for Phase 3, Study of the Effects of VHSV

Catalyst amount and feed flowrates of both ethanol and water were varied in order to manipulate VHSV throughout phase 3. Limitations were found with pump minimum flowrate as well as minimum and maximum catalyst amounts. There was also a maximum ethanol flowrate based on cost. Runs typically lasted upward of 300 minutes, using greater than 1.5 mL/min was not feasible. The largest reactor available could hold a maximum of 1.6 grams of catalyst. A much smaller reactor was used for liquid phase trials. A minimum catalyst amount of 0.02 grams was needed to ensure that some sort of packed bed existed within the reactor. The highest liquid phase VHSV achievable with 0.02 grams of catalyst and the maximum ethanol flowrate was 24.35. In order to reach higher VHSVs, catalyst amount was decreased to 0.01 grams and mixed with 10 grams of sand.

3.5 Volume-Hourly Space Velocity

Volume-hourly space velocity (VHSV) was used as the basis to compare vapor and liquid phase reactions. VHSV accounts for the difference in density between the two phases. With ethanol, the difference between liquid phase and vapor phase density is 3 orders of magnitude. Liquid phase density at 400°C is 0.91 g/mL, while vapor density is 0.000332 g/mL. Comparison based on VHSV ensures that the same volume of reactant is encountering the same volume of catalyst. VHSV is calculated with the following formula:

$$\text{VHSV} = \frac{\dot{V}_{\text{EtOH}}}{\text{volume catalyst}}$$

The volumetric flowrate of ethanol is divided by the volume of catalyst. VHSV provided an accurate basis to compare differences between liquid and vapor phase ethanol dehydration.

3.6 Ethanol Conversion

A calibration curve was used to determine the amount of weight percent of ethanol present in liquid product samples. From there the moles of unreacted ethanol, and therefor also reacted moles of ethanol were found and compared to the moles of reactant that were fed into the process over the sampling time. Conversion percent was calculated according to the following formulas:

$$Peak\ Area = 5136018.83 * Ethanol\ Weight\ Percent + 44344.32$$

$$Ethanol\ Mole\ Percent = \frac{\frac{Ethanol\ Weight\ Percent}{Ethanol\ Molar\ Mass}}{\frac{Ethanol\ Weight\ Percent}{Ethanol\ molar\ Mass} + \frac{100 - Ethanol\ Weight\ Percent}{Water\ Molar\ Mass}}$$

$$Conversion = 100 - (100 * Ethanol\ Mole\ Percent)$$

An important assumption made for this calculation is that the liquid products consist only of water and ethanol. This assumption is valid when there is very little ethanol detected in the liquid product sample. For a true conversion value, all liquid products would need to be factored into the denominator of the mole percent calculation.

3.6 Ethylene Yield

Ethylene yield was also calculated based on quantity of ethylene determined through the use of a calibration curve. Volume percent of ethylene was found. It was assumed that the remaining volume in the sample loop was filled with nitrogen, the carrier gas. From this information, flowrate of ethylene was found in milliliters per minute and then converted to moles per minute. The molar flowrate of ethylene was then divided by the molar flowrate of ethanol to determine yield. The following series of formulas were used for this calculation:

$$Peak\ Area = 4330218.9 * Ethylene\ Volume - 5414486.67$$

$$Volume\ \%\ Etylene = \frac{Ethylene\ Volume}{Sample\ Loop\ Volume}$$

$$Volume\ \%\ Nitrogen = 1 - Volume\ \%\ Ethylene$$

$$Flowrate\ Ethylene = \frac{Nitrogen\ Flowrate - (Volume\ \%\ Nitrogen * Nitrogen\ Flowrate)}{Volume\ \%\ Nitrogen}$$

$$Yield = \frac{Flowrate\ Ethylene}{Flowrate\ Ethanol} * 100$$

The assumption made in this step is dependent on the ethylene volume percent being very small relative to nitrogen volume percent. The assumption breaks down at nitrogen volume percentages less than 90%.

Chapter 4: Results

This portion of the report will detail the results of extensive data analysis. All experimental runs contributed to the learning outcomes of this study, however the final 12 trials were the most illuminating. The following sections on yield, selectivity and throughput focus heavily on the last 12 trials where VHSV became a basis for comparison.

4.1 Gaseous Products

Gaseous products were analyzed with the in-line GC-FID. Liquid phase ethanol dehydration product peaks were very distinct. Figure 12 below shows the results of one GC injection in the liquid phase, after steady state was achieved.

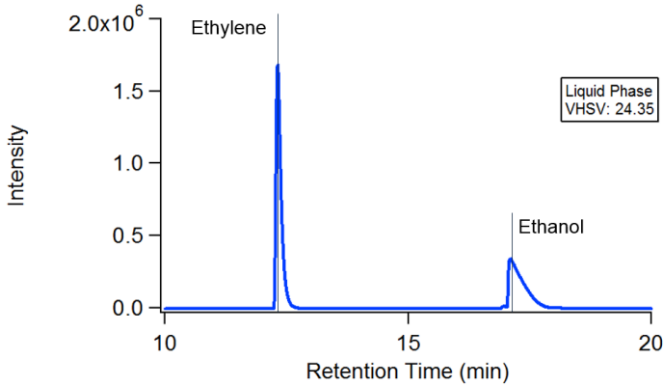

Figure 12: Liquid Phase Steady State Gaseous Products

Only two peaks were observed in products of liquid phase ethanol dehydration, ethylene and ethanol. The presence of ethanol in the gaseous products indicates that liquid phase ethanol dehydration does not reach 100% conversion. Having only two gaseous products makes product separation very simple. The ethanol in the gas product can easily be condensed to produce nearly pure ethylene.

Vapor phase ethanol dehydration produces more varied products. Figure 13 below shows typical steady state results of one injection from the vapor phase reaction.

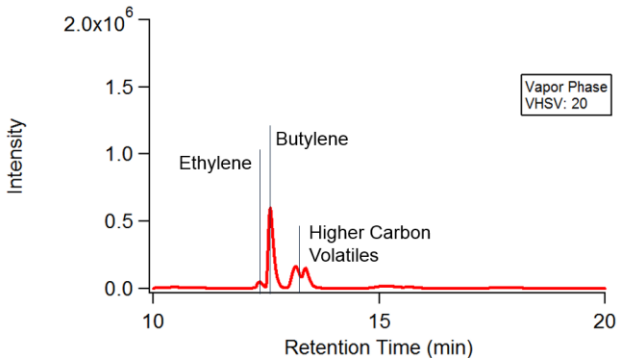

Figure 13: Vapor Phase Steady State Gaseous Products

Vapor phase ethanol dehydration produces various carbon volatiles at low VHSVs. The most abundant product is butylene. For this study ethylene was the product of interest. The reaction would not be run this slowly under vapor phase conditions industrially to produce ethylene. Higher carbon volatiles are present because of the long amount of time it takes for the reactant to proceed through the packed bed reactor. The non-distinct peak after a retention time of 13 minutes contains products that could not be identified with the GC-FID method that was used. The peaks colluded making it difficult to definitively identify the additional products. Another feature to note is the absence of an ethanol peak. Vapor phase ethanol dehydration showed very high conversion, so much so that ethanol was not detected in the gaseous product.

Liquid phase ethanol dehydration at the VHSVs studied shows a clear advantage. The overlay below illustrates the differences between the phases very clearly.

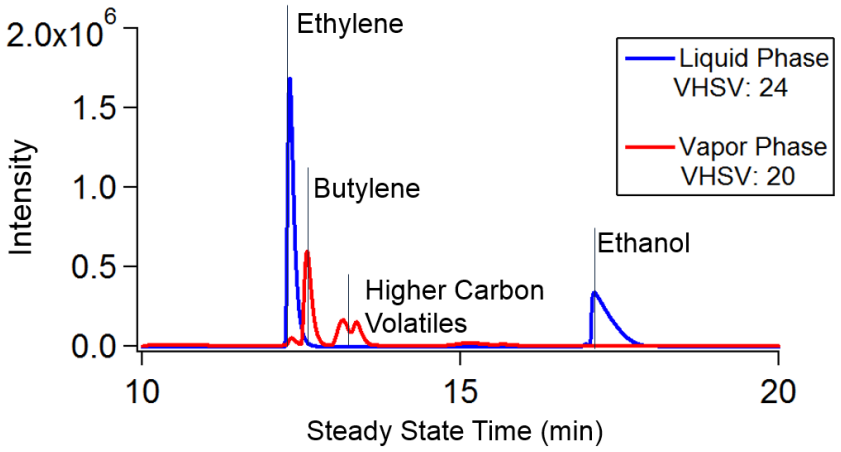

Figure 14: Overlay of Steady State Gaseous Products

It is clear that liquid phase ethanol dehydration, under these conditions, produces much greater amount of ethylene. Vapor phase ethanol dehydration produces a more varied product set. While the peaks labelled “Higher Carbon Volatiles” could not be identified, with gas chromatography compounds that have a greater molar mass have a longer retention time. Compounds with similar molar masses produce a peak at similar times. All of the products from vapor phase ethanol dehydration are observed from 2-3.5 minutes. This suggests that all products have a relatively similar molar mass and would not be easily separated. Liquid phase generates more ethylene. Liquid phase ethanol dehydration is also more selective toward ethylene production versus higher carbon volatiles.

4.2 Liquid Products

Liquid products were also collected from all runs. Similar to gas products, liquid and vapor phase reactions produced different liquid products. Liquid phase ethanol dehydration produced a homogenous solution largely consisting butanol, ethanol and water. GC-MS was used to identify the components of the liquid products and then GC-FID was used for each sample to determine conversion of ethanol and yield of butanol. Figure 15 below shows the GC-MS identification of liquid products.

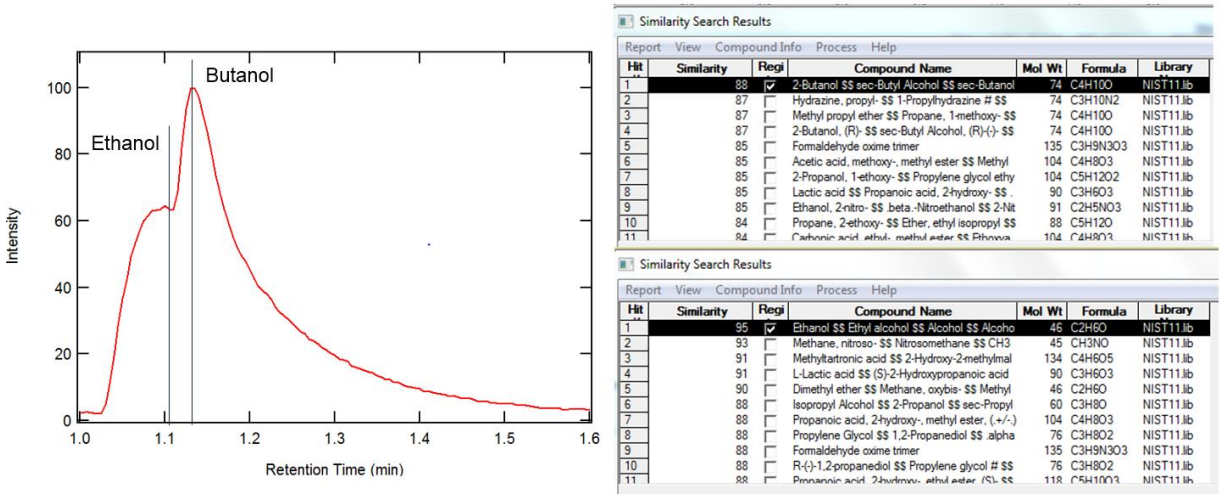

Figure 15: GC-MS Identification of Liquid Products

GC-MS identified the first peak as ethanol with a similarity of 95, and the second peak as butanol with a similarity of 88. The column and method used for the GC-MS were not able to fully separate ethanol and butanol. GC-FID was more appropriate to separate and determine the

amounts of each component. A representative GC-FID analysis of the liquid product is shown below in Figure 16.

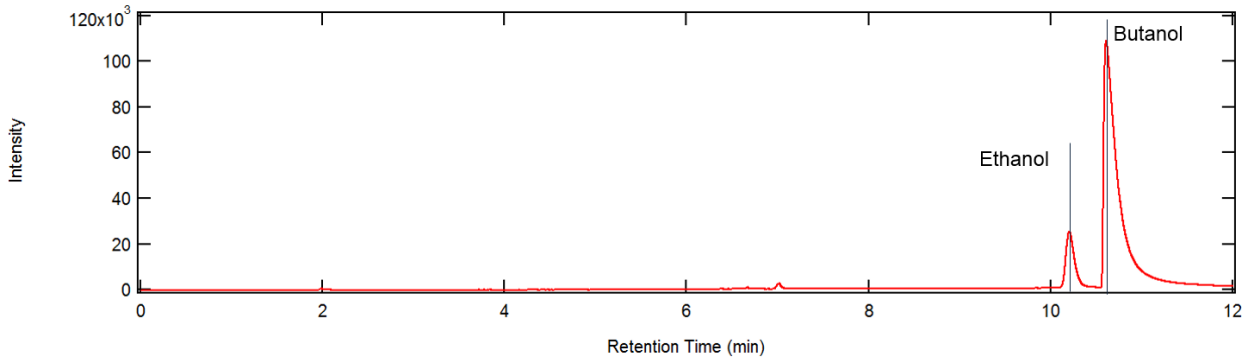

Figure 16: GC-FID Analysis of Liquid Products

Both the injections analyzed in Figure 15 and 16 are from the same liquid sample. GC-FID was able to separate the components and produce distinct peaks that could then be used for further analysis.

Vapor phase reactions produced the same homogeneous polar mixture with an oil layer at the top. A typical sample from vapor phase ethanol dehydration is shown below in Figure 17.

Figure 17: Typical Liquid Product from Vapor Phase Ethanol Dehydration

More oil was produced during the early phase of the reaction. As the reaction proceeded, less oil was produced. Samples collected at the end of vapor phase trials did not have an oil component. This suggests that pathway for oil production is blocked as the reaction proceeds and the zeolite lattice changes. Oil samples were analyzed with GC-MS producing the following results shown below in Figure 18.

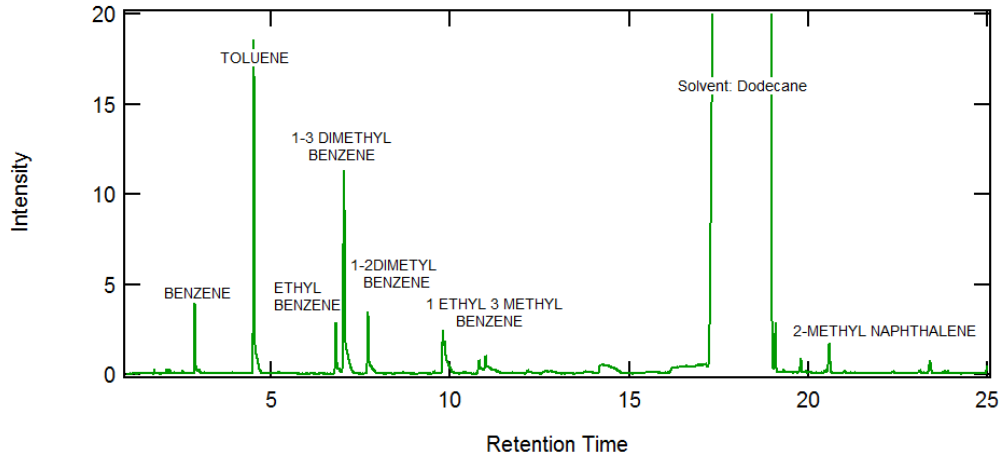

Figure 18: Oil Sample GC-MS Analysis

The non-polar, oily component of the liquid products from vapor phase ethanol dehydration are largely a mix different benzene aromatics. Dodecane was selected as the solvent for GC-MS testing as it did not interfere with the majority of product peaks generated.

4.3 Reaction Activity

Reaction activity patterns varied between the gas and liquid phase reactions. Eventually, reactions in both phases would reach steady state.

4.3.1 Liquid Phase Ethanol Dehydration Reaction Activity

Liquid phase reactions generally followed a distinct pattern. Figure 19 below shows a typical example of a liquid phase reaction.

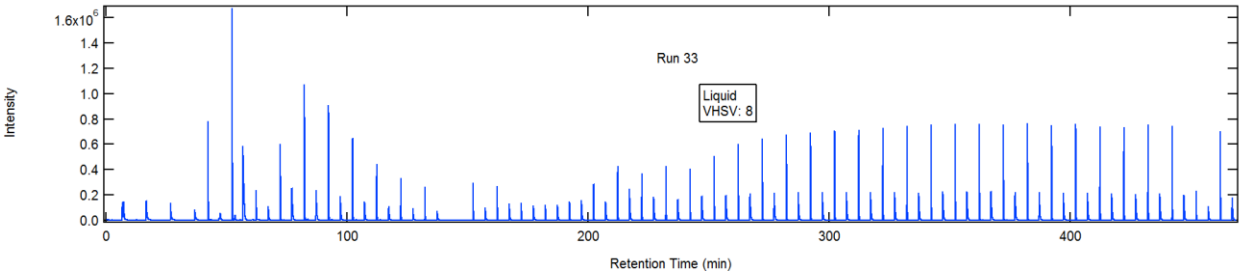

Figure 19: Typical Liquid Phase Reaction Activity from In-Line GC-FID

Liquid phase reactions typically exhibited a short ramp up period, followed by a spike in activity and then decline. The sharp decline is then followed by another ramp up period resulting in steady state. The above intensity graph was generated from a trial with a VHSV of 8. The

patterns observed in reaction activity are more apparent in trials at slower VHSVs. Figure 20 below shows the GC-FID results for a reaction at a VHSV triple that in Figure 19.

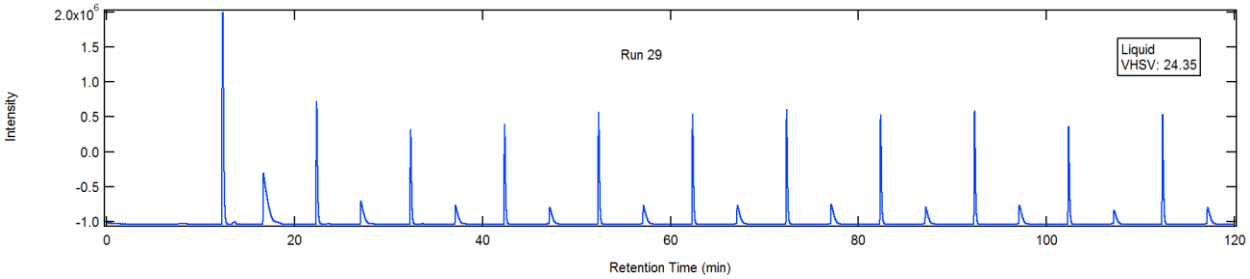

Figure 20: Liquid Phase Reaction with VHSV of 24.35

The pattern described above is not seen at faster VHSVs. It is likely that the reaction proceeds in a similar fashion, but the GC injections are not frequent enough to capture data points to illustrate the pattern. Timing between GC injections is dependent upon the compounds being measured. With the column and method used for this study ethylene peaks are observed between 2.3 and 2.6 minutes. Ethanol peaks are seen in the 7 minute range. To observe the pattern at faster VHSVs a different method of analysis or type of equipment would be needed.

4.3.2 Vapor Phase Ethanol Dehydration Reaction Activity

Vapor phase ethanol dehydration did not exhibit a reliable pattern of activity. No products were detected for a long period of time and then a quick ramp up would occur leading to a period of high activity, followed by relatively steady state. The period of time before products were detected was a direct result of the flowrates of the reactants and VHSV. Figure 21 below shows how VHSV effected product detection.

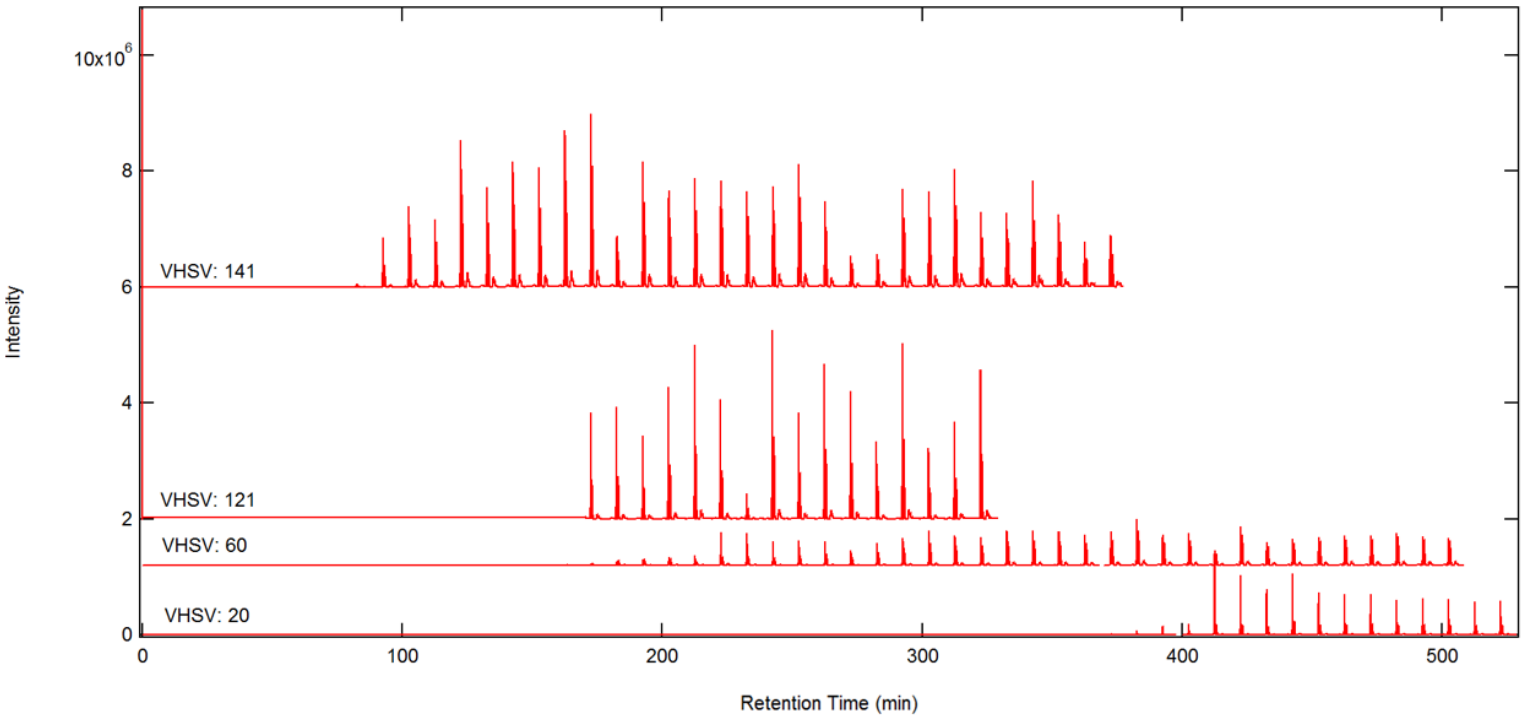

Figure 21: Vapor Phase Reaction Activity from In-Line GC-FID

At low VHSVs, products were not detectable for an extended period of time. The reactants took a long time to move through the packed bed reactor- as the trials were run at atmospheric pressure. This extended period of time without products is non-ideal for an industrial setting. VHSV greatly affected this amount of time. VHSV also contributed to the gross amount of products generated. While higher VHSVs produced generated more products sooner after start-up these results may not be viable for industry. Intensity charts for all trials involved in the VHSV comparison can be found in Appendix E.

4.3.3 Steady State

Steady state was reached in most experimental trials. For the purposes of this project, steady state was defined as 60 minutes where the major products peak intensity varied by less than 10%. Liquid phase ethanol dehydration consistently exceeded this definition. Steady state lasted significantly longer than 60 minutes for many liquid phase trials. This definition had to be expanded for vapor phase trials. Especially at lower VHSVs, products were not consistent. If there was not a clear period of steady state production, a representative portion of the data set was used. Once a steady state region or representative data set was identified, peak area for each product was averaged. This average peak area was then used for further analysis.

4.4 Conversion

Both liquid and vapor phase ethanol dehydration showed very high conversion rates. Conversion was calculated based on liquid product analysis. Liquid product samples were collected periodically throughout a trial. Each sample underwent GC-FID analysis, results from all sample for each trial were averaged to determine total conversion. Figure 22 below shows average ethanol conversion from each trial of both liquid and vapor phase ethanol dehydration.

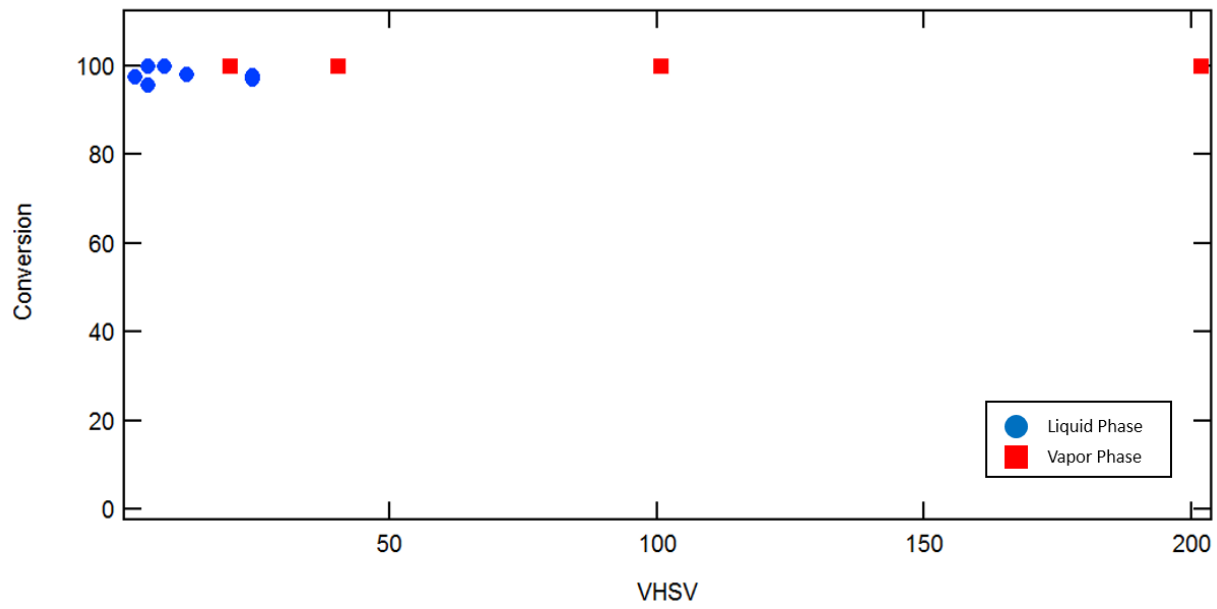

Figure 22: Ethanol Conversion

Vapor phase consistently showed 100% ethanol conversion at all VHSVs. Liquid phase reactions also showed very high conversion, typically between 95 and 98 percent. Raw data for conversion calculation can be found in Appendix G.

4.5 Yield

From the average steady state peak area, yield was calculated. A calibration curve was generated for ethylene, butanol, and ethanol. The calibration curves for each of these can be seen found in Appendix C. From the calibration curve, the amount of each product was determined. The amount of product could then be used to calculated yield. The raw data for yield calculation can be found in Appendix G: Raw Data. When plotted against VHSV, ethylene yield follows a distinct trend. This can be seen below in Figure 23:

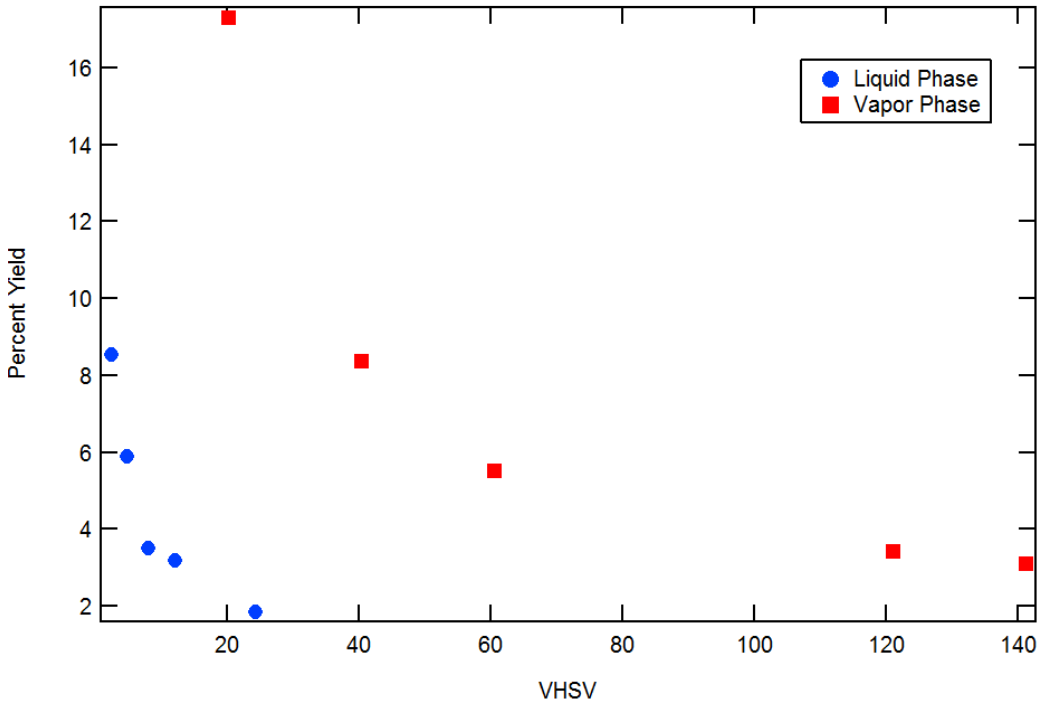

Figure 23: Ethylene Yield

In both phases, ethylene percent yield was greatest at low VHSVs. As VHSV was increased, ethylene yield asymptotically decreased toward zero percent. Although ethanol conversion in both phases was fairly high, ethylene percent yield was always less than 20%.

The most prevalent other major product was butanol. Butanol yield was found through analysis of the liquid products of both reaction phases. Figure 24 and 25 below show butanol and ethylene yield from liquid and vapor phase ethanol dehydration respectively.

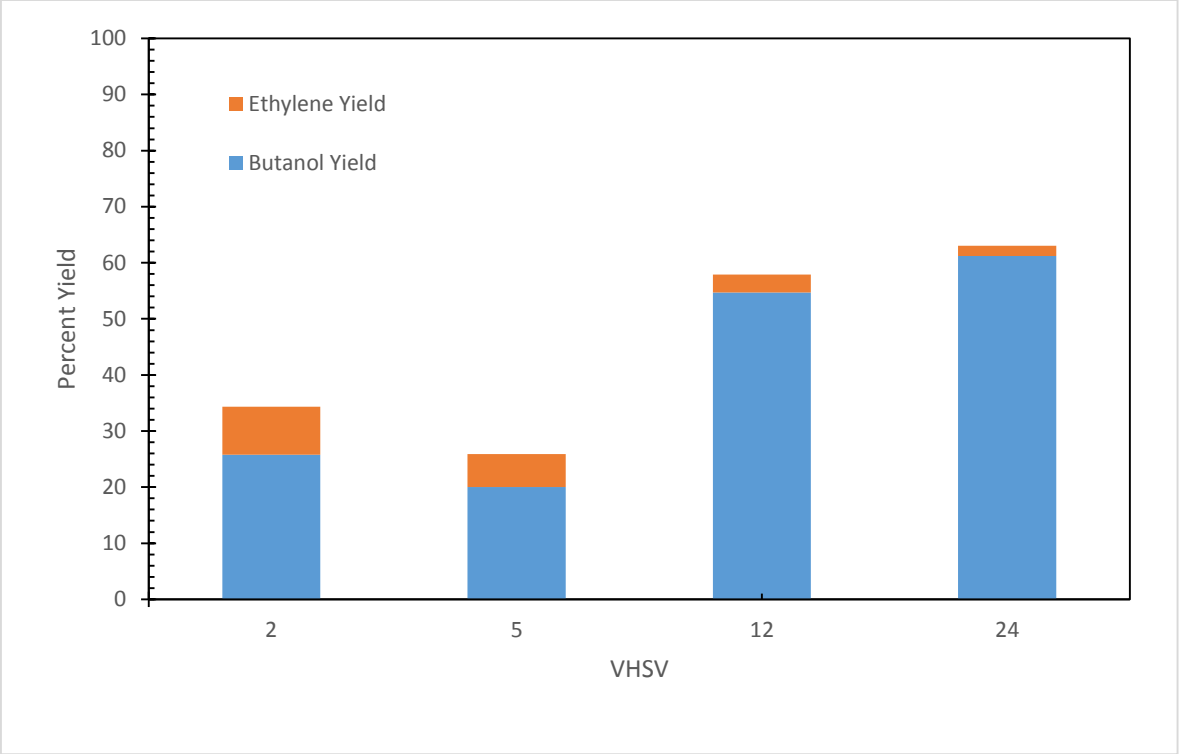

Figure 24: Liquid Phase Product Yield

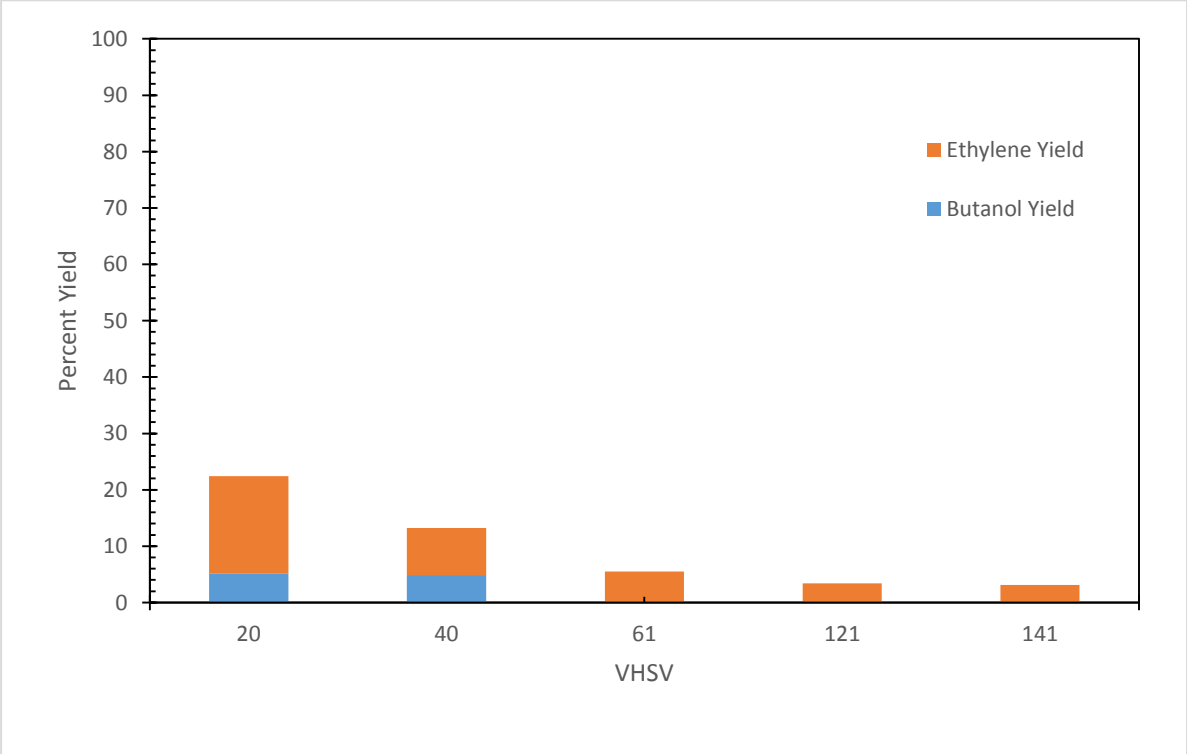

Figure 25: Vapor Phase Product Yield

Liquid phase ethanol dehydration produces considerably more butanol than ethylene. Butanol yield increases with VHSV as ethylene yield decreases. A different phenomena is observed in vapor phase ethanol dehydration. Butanol yield decreases along with ethylene yield as VHSV increases. At VHSVs above 50, butanol is not observed as a product. Vapor phase total product yield is notably less than that of liquid phase ethanol dehydration. The additional products are higher carbon volatiles as discussed above. Those peaks could not be separated well or identified, therefor no yield data is available for the additional gaseous products.

4.6 Throughput

Analysis of average steady state ethylene peak area per gram of catalyst shows a significant advantage to liquid phase ethanol dehydration. In order to achieve the VHSVs used in this study, vapor phase trials used 80 times the amount of zeolite than the liquid phase trials. The graph in Figure 26 below show average steady state peak area per gram of catalyst.

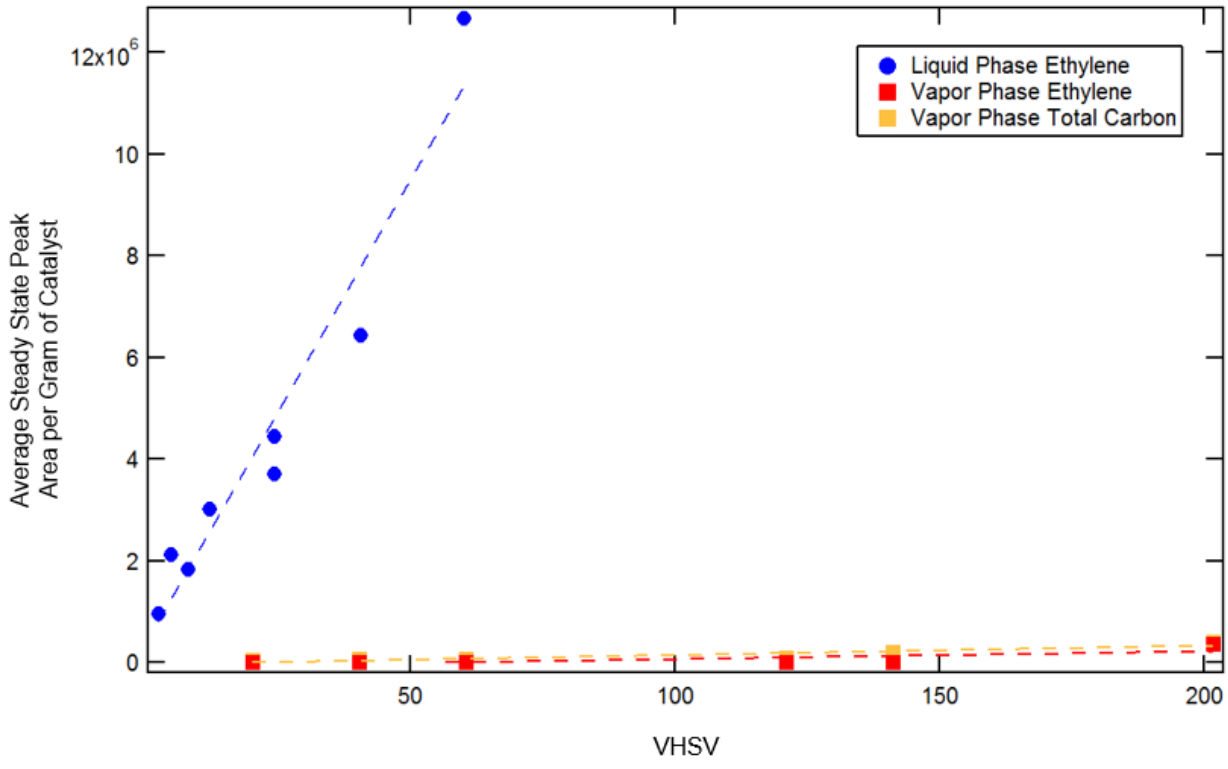

Figure 26: Throughput Comparison based on VHSV

Liquid phase ethylene production is shown in blue, vapor phase is shown in red. The additional yellow line includes the total carbon gaseous products that were present in the GC-FID. A table

in Appendix G: Raw Data. At the flowrates/VHSVs studied, liquid phase ethanol dehydration produces a significantly greater amount of ethylene. Even when considering the higher carbon volatiles, liquid phase ethanol dehydration produces more products.

Revisiting the idea of VHSV versus WHSV, liquid phase ethanol dehydration also shows a throughput advantage when WHSV is used as the basis for comparison. Figure 27 below show yield percent per gram of catalyst compared on the basis of VHSV and WHSV.

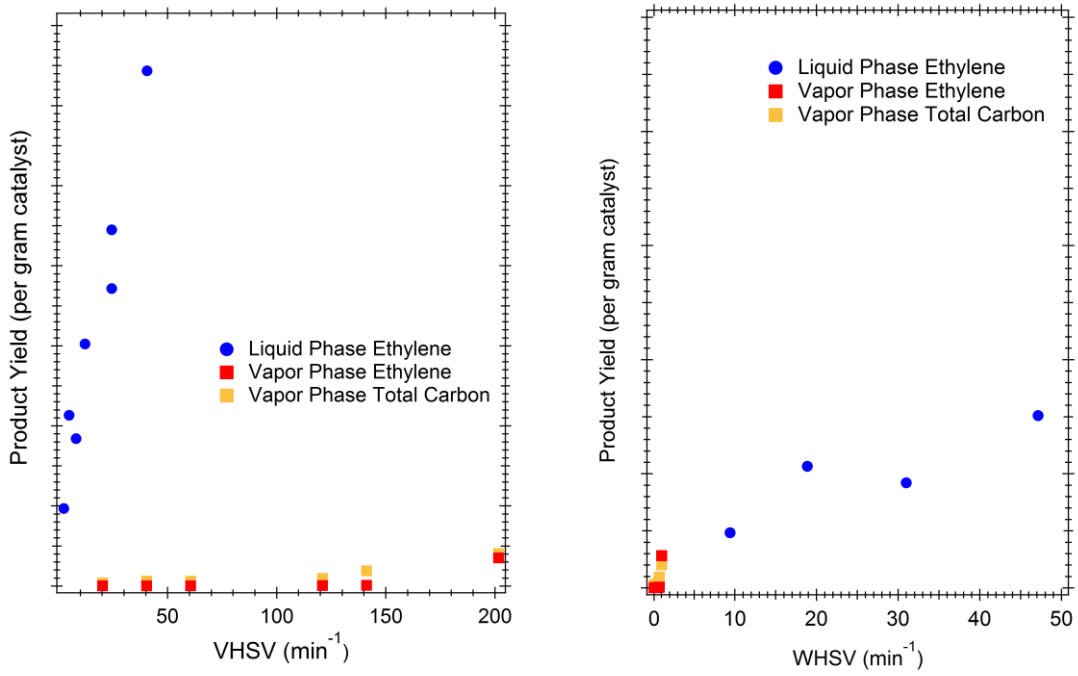

Figure 27: WHSV and VHSV Comparison

When ethanol dehydration in both liquid and vapor phase are compared based on mass flowrate, liquid phase reactions show a significant advantage. More ethanol is being fed into the reaction, producing more ethylene, using less catalyst.

Chapter 5: Conclusions and Recommendations

5.1 Conclusions

From the data analysis discussed above, conclusions can be drawn about the advantages of liquid phase ethanol dehydration.

1. Liquid phase ethanol dehydration shows comparable conversion to the vapor phase. An insignificant amount of ethanol is found in the gaseous products and virtually no ethanol is found in the liquid products.
2. At low volume hourly space velocities, liquid phase ethanol dehydration produces more ethylene and butanol than vapor phase reactions. Liquid phase ethanol dehydration also produces a large amount of butanol.
3. On a per gram of catalyst basis, liquid phase ethanol dehydration shows a massive advantage in ethylene production over vapor phase reactions.

The conclusions reached by this study have great industrial potential. Liquid phase ethanol dehydration can address some of the challenges presented by traditional, vapor phase bio-ethanol dehydration.

5.1.1 Industrial Considerations

Liquid phase ethanol dehydration has many industrial advantages over vapor phase ethanol dehydration that is current common practice. The one major disadvantage is that in order to operate in the liquid phase, the reactor must be run at very high pressures (2800-3600 psi). High pressure operations presents a safety issue. Equipment must be designed to handle the pressure and additional safety measures must be taken. Operators require additional training, and personal protective equipment and shields must be provided. However, once the initial capital investment is made for safety equipment, running at high pressure and 390°C is more cost effective than running at the very high temperature that Braskem does.

The industrial advantages of liquid phase ethanol dehydration arguably outweigh the disadvantages. Liquid phase ethanol dehydration yields very good results with a feed that is not 100 percent ethanol. Often the broth from the fermentation process that produces bio-ethanol is a “wet” broth, meaning it has high water content. Before traditional vapor phase catalytic dehydration can occur, the broth needs to be dried substantially, removing most of the water.

This study has shown that at a 2:1 ethanol to water feed ratio liquid phase dehydration produces a large amount of ethylene. In industry, use of liquid phase dehydration would eliminate the need for equipment and process steps associated with drying the fermentation broth. Elimination of this step is also a time saving measure.

The reduced amount of catalyst needed to operate at low volume hourly space velocities is also attractive to industry. The liquid phase reactions in this study used 80 times less catalyst than the vapor phase runs. The catalyst is destroyed throughout the reaction, so using less catalyst to begin with presents a cost advantage. Reactor size can also be reduced to accommodate the smaller packed bed size needed.

Additionally, liquid phase ethanol dehydration products are more easily separated than those of vapor phase. Fewer products are produced to begin with. Upon exiting the reactor, separation naturally occurs between liquid and gaseous products. The only products detected in the gas phase are ethylene and ethanol. At atmospheric pressure, the difference in boiling point between ethylene and ethanol is nearly 200°C (-103.7°C and 78.4°C respectively). A large difference in boiling point allows for easy separation. Vapor phase ethanol dehydration produces many gas phase products with similar molecular weights. The molecular weights of the compounds referred throughout this report as “higher carbon volatiles” are so similar that they could not be separated by a gas chromatograph specifically designed for separation. The products from vapor phase ethanol dehydration require several separation steps to isolate ethylene, the desired product.

5.2 Recommendations for Further Study

Further investigation of a greater range of volume-hourly space velocities for ethanol dehydration in both liquid and vapor phase would make the evidence more compelling. In this study, experimental limitations were found with pump flowrate minimums and maximums and reactor size. The cost of ethanol also became cost prohibitive at higher flowrates. Further development of a GC-FID method capable of separating the gaseous products from vapor phase ethanol dehydration would also be useful. Identification and quantification of those products would close the carbon balance and allow for a better understanding of the reaction. Additional calibration curves would also need to be created for this further analysis.

Acknowledgements

The project team thanks Professor Michael Timko, our advisor, for his constant encouragement and ability to direct us in this project. Additionally, we would like to thank Alex Maag, a chemical engineering PhD Candidate, for the countless hours of assistance inside the laboratory and for the support with research and data analysis outside of the laboratory.

References

Brazilian Sugarcane Industry Association. *Sugarcane Producing Regions in Brazil*. Unica, n.d. Web. 28 Sept. 2015. <http://english.unica.com.br/production-map/>.

Cameron, G., Le, L., Levine, J., & Nagulapalli, N. (2012, April 1). Process Design for the Production of Ethylene from Ethanol. Retrieved November 9, 2015, from http://repository.upenn.edu/cgi/viewcontent.cgi?article=1036&context=cbe_sdr

Chen, Yu, Zhen Chen, Yulong Wu, Ling Tao, Bin Dai, Mingde Yang, and Xiaoyan Zhu. 2010. Dehydration reaction of bio-ethanol to ethylene over modified SAPO catalysts.*Journal of Industrial and Engineering Chemistry* 16 (5): 717-22.

Fan, Denise, Der-Jong Dai, and Ho-Shing Wu. "Ethylene Formation by Catalytic Dehydration of Ethanol with Industrial Considerations." *Materials* 6 (2013): 101-15. Web.

Fogler, H. Scott. *Elements of Chemical Reaction Engineering*. 4th ed. Upper Saddle River, NJ: Prentice Hall PTR, 2005. Print. p.645-755

Haro, P., P. Ollero, and F. Trippe. "Technoeconomic Assessment of Potential Processes for Bio-Ethylene Production." *Fuel Processing Technology* 114 (2013): 35-48. Web.

Lisensky, George. 2010. "Preparation of Zeolite ZSM5 and Catalysis of Xylene Isomerization" *University of Wisconsin-Madison MRSEC Education Group*. 2010. Web. 13 Nov 2015. http://education.mrsec.wisc.edu/nanolab/zeolite/

Luiz, Paulo, Augusto Morita, Luis F. Cassinelli, Antonio Morschbacker, and Roberto Werneck Do Carmo. "Braskem's Ethanol to Polyethylene Process Development." *Catalytic Process Development for Renewable Materials* 1 (2013): 149-65. Web.

Phillips, Cory B., and Ravindra Datta. "Production of Ethylene from Hydrous Ethanol on H-ZSM-5 under Mild Conditions." *Industrial & Engineering Chemistry Research* 36 (1997): 4466-475. - *Industrial & Engineering Chemistry Research (ACS Publications)*. Web. 18 Jan. 2016. <http://pubs.acs.org/doi/pdf/10.1021/ie9702542>.

Plant Bottle Frequently Asked Questions. *The Coca-Cola Company- Plant Bottle FAQ*. N.p., n.d. Web. 28 Sept. 2015. <http://www.coca-colacompany.com/plantbottle-technology/plantbottle-frequently-asked-questions#TCCC>.

Ravenelle, Ryan M., Florian Schübler, Andrew Damico, Nadiya Danilina, Jeroen A. Van Bokhoven, Johannes A. Lercher, Christopher W. Jones, and Carsten Sievers. 2010. Stability of Zeolites in Hot Liquid Water. *Journal of Physical Chemistry C* 114 (46): 19582-95.

Sadaba, Irantzu, Manuel Lopez Granados, Anders Riisager, and Esben Taarning. "Deactivation of Solid Catalysts in Liquid Media: The Case of Leaching of Active Sites in Biomass Conversion Reactions." *Green Chemistry* 17.8 (2015): 4133-145. *Publishing: Journals, Books, and Databases*. Web. <http://pubs.rsc.org/en/Content/ArticleLanding/2015/GC/C5GC00804B#!divAbstract>.

What is Catalysis? *North American Catalysis Society*. February, 2008. Web. 26 Mar. 2016. http://nacatsoc.org/above/what-is-catalysis/

What is throughput? *Business Dictionary*. 2016. Web. 20 Mar 2016. http://www.businessdictionary.com/definition/throughput.html

Williams, J. (2010, February 1). Bioplastics: Renewable Materials Factsheet. Retrieved November 9, 2015, from http://www.nnfcc.co.uk/publications/nnfcc-renewable-polymers-factsheet-bioplastics

Zeolites. *Chemistry Explained: Foundations and Applications*. 2016. Web. 26 Mar 2016. http://www.chemistryexplained.com/Va-Z/Zeolites.html

Zhang, Xian, Rijie Wang, Xiaoxia Yang, and Fengbao Zhang. "Comparison of Four Catalysts in the Catalytic Dehydration of Ethanol to Ethylene." *Microporous and Mesoporous Materials* 116.1-3 (2008): 210-15. *Science Direct*. Web. 28 Sept. 2015. <http://www.sciencedirect.com/science/article/pii/S1387181108001819>.

Appendix A: Zeolite ZSM-5 Material Safety Data Sheet

ZEOLYST INTERNATIONAL

MSDS
MATERIAL SAFETY DATA SHEET

Trade Name: **CBV2314**
ZEOLITE AMMONIUM ZSM-5 POWDER
Date Prepared: 03/14/06 *Page:* 1 of 4

1. CHEMICAL PRODUCT AND COMPANY IDENTIFICATION

Product name:	CBV2314
Product description:	ZEOLITE AMMONIUM ZSM-5 POWDER
Manufacturer:	Zeolyst International P. O. Box 830 Valley Forge, PA 19482 USA
Telephone:	610-651-4200
In case of emergency call:	610-651-4200
For transportation emergency Call CHEMTREC:	800-424-9300

2. COMPOSITION/INFORMATION ON INGREDIENTS

Chemical and Common Name	*CAS Registry Number*	*Wt. %*	*OSHA PEL*	*ACGIH TLV*
Zeolite	1318-02-1	100%	15mg/m^3 total dust 5mg/m^3 respirable (Particulates Not Otherwise Regulated)	10 mg/m^3 3 mg/m^3 respirable

3. HAZARDS IDENTIFICATION

Emergency Overview:	White, odorless, powder. Causes respiratory irritation. Causes mild eye irritation. May cause skin irritation. Ammonia released on contact with strong bases. Noncombustible. Ammonia or nitrogen oxides may be released at high temperatures.
Eye contact:	Causes mild eye irritation.
Skin contact:	Prolonged or repeated contact may dry skin and cause irritation.
Inhalation:	Causes irritation.
Ingestion:	No known hazards. Inedible.
Chronic hazards:	No known hazards.
Physical hazards:	Absorbs water from air and fluids. Generates heat when it absorbs water.

4. FIRST AID MEASURES

Eye:	In case of contact, immediately flush eyes with plenty of water for at least 15 minutes. Get medical attention if irritation persists.
Skin:	In case of contact, immediately flush skin with plenty of water. Remove contaminated clothing and shoes. Get medical attention if irritation develops

	and persists. Wash clothing before reuse. Thoroughly clean shoes before reuse.
Inhalation:	Remove to fresh air. If not breathing, give artificial respiration. If breathing is difficult, give oxygen. Get medical attention.
Ingestion:	Not applicable.

5. FIRE FIGHTING MEASURES

Flammable limits:	This material is noncombustible.
Extinguishing Media:	This material is compatible with all extinguishing media.
Hazards to fire-fighters:	Ammonia or nitrogen oxides may be released at high temperatures.
Fire-fighting equipment:	The following protective equipment for fire fighters is recommended when this material is present in the area of a fire: self-contained breathing apparatus (SCBA), chemical goggles, body-covering protective clothing, chemical resistant gloves, and rubber boots.

6. ACCIDENTAL RELEASE MEASURES

Personal protection:	Wear safety goggles, body-covering protective clothing, chemical resistant gloves, and rubber boots, NIOSH-approved dust respirator where dust occurs. See section 8.
Environmental Hazards:	Sinks in water. No know environmental hazards.
Small spill cleanup:	Carefully shovel or sweep up spilled material and place in suitable container. Avoid generating dust. Use appropriate Personal Protective Equipment (PPE). See section 8.
Large spill cleanup:	Keep unnecessary people away; isolate hazard area and deny entry. Do not touch or walk through spilled material. Carefully shovel or sweep up spilled material and place in suitable container. Avoid generating dust. Use appropriate Personal Protective Equipment (PPE). See section 8.
CERCLA RQ:	There is no CERCLA Reportable Quantity for this material. If a spill goes off site, notification of state and local authorities is recommended.

7. HANDLING AND STORAGE

Handling:	Avoid contact with eyes, skin and clothing. Avoid breathing dust. Keep container closed. Promptly clean up spills. Wash thoroughly after handling.
Storage:	Keep containers closed. Store separated from strong bases in original containers or clean metal, plastic, or fiber containers.

Appendix B: Gas Chromatograph Methods

GC-FID Gaseous Product Analysis Method		
AOC-20i		
Injection Volume		1.0 µL
# of Rinses with Solvent (Pre-run)		0
# of Rinses with Solvent (Post-run)		0
# of Rinses with Sample		1
Plunger Speed (Suction)		High
Viscosity Comp. Time		0.2 sec
Plunger Speed (Injection)		High
Syring Injection Speed		High
Injection Mode		Normal
SPL2		
Temperature		250°C
Injection Mode		Split
Sampling Time		1.00 min
Flow Control Mode		Pressure
Pressure		11.1 psi
Total Flow		13.0 mL/min
Column Flow		1.67 mL/min
Linear Velocity		33.1 cm/sec
Purge Flow		3.0 mL/min
Split Ratio		5
Column Name		Rt-U-BOND
Film Thickness		0.10 µm
Length		30.0 m
Inner Diameter		0.32 mm
Column		
Temperature		130°C
Equilibrium Time		0.5 min
Column Oven Temperature Program		
Rate	Temperature	Hold Time
-	130	410.00
FID1		
Temperature		250°C
Sampling Rate		40 msec
Stop Time		410 min
Delay Time		0.00 min
Subtract Detector		None
Flow Program		Makeup
Column Oven Temperature Program		
Rate	Flow	Hold Time
-	30	0.00

Figure 28: GC-FID In-Line Method for Gaseous Product Analysis

GC-FID Liquid Product Analysis Method		
AOC-20i		
Injection Volume		1.0 µL
# of Rinses with Solvent (Pre-run)		0
# of Rinses with Solvent (Post-run)		0
# of Rinses with Sample		1
Plunger Speed (Suction)		High
Viscosity Comp. Time		0.2 sec
Plunger Speed (Injection)		High
Syring Injection Speed		High
Injection Mode		Normal
SPL2		
Temperature		250°C
Injection Mode		Split
Sampling Time		1.00 min
Flow Control Mode		Pressure
Pressure		11.1 psi
Total Flow		16.7 mL/min
Column Flow		2.29 mL/min
Linear Velocity		37.6 cm/sec
Purge Flow		3.0 mL/min
Split Ratio		5
Column Name		Rt-U-BOND
Film Thickness		0.10 µm
Length		30.0 m
Inner Diameter		0.32 mm
Column		
Temperature		60°C
Equilibrium Time		0.5 min
Column Oven Temperature Program		
Rate	Temperature	Hold Time
-	60	1.00
10.00	150	2.00
FID1		
Temperature		250°C
Sampling Rate		40 msec
Stop Time		12 min
Delay Time		0.00 min
Subtract Detector		None
Column Oven Temperature Program		
Rate	Flow	Hold Time
-	30	0.00

Figure 29: GC-FID Method for Liquid Product Analysis

GC-Mass Spectrometer Method for Compound Identification		
Sampler		
# of Rinses with Solvent (Pre-run)		0
# of Rinses with Solvent (Post-run)		1
# of Rinses with Sample		2
Plunger Speed (Suction)		High
Viscosity Comp. Time		0.2 sec
Plunger Speed (Injection)		High
Syring Injection Speed		High
Injection Mode		0: Normal
GC		
Column Oven Temp		40°C
Injection Temp		90°C
Injection Mode		Split
Row Control Mode		Linear Velocity
Pressure		21 psi
Total Flow		9.0 mL/min
Column Flow		2.66 mL/min
Linear Velocity		58.8 cm/sec
Purge Flow		1.0 mL/min
Split Ratio		2
Column Name		SHRXI-5MS
Thickness		0.25 µm
Length		30.0 m
Diameter		0.25 mm
GC Program		
Rate	Final Temp	Hold Time
-	40	1.00
2.00	60	0.00
MS		
Ion Source Temp		230°C
Interface Temp		75°C
Solvent Cut Time		0.1 min
Micro Scan Width		0
GC Program Time		11 min

Figure 30: GC-MS Method for Compound Identification

Appendix C: Gas Chromatograph Calibration Curves

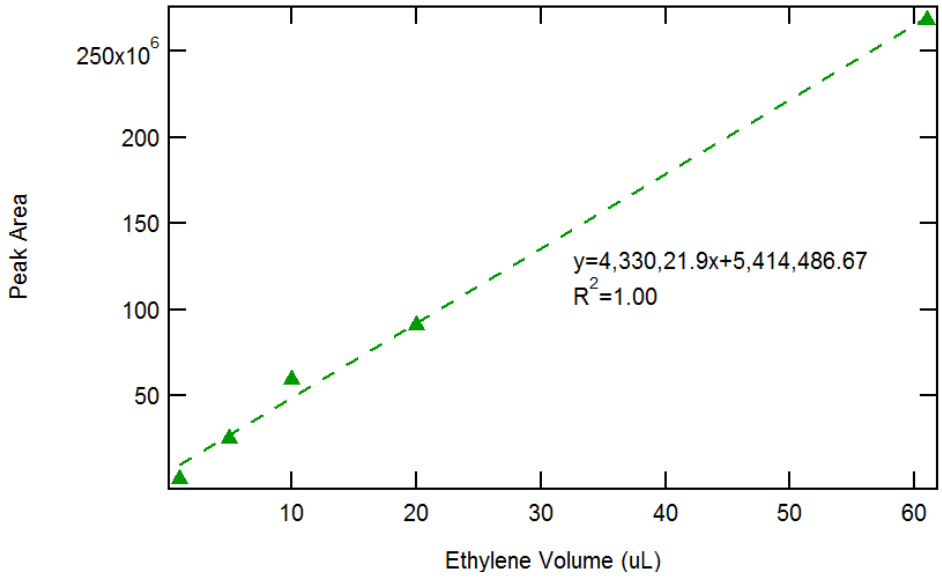

Figure 31: Ethylene Calibration Curve

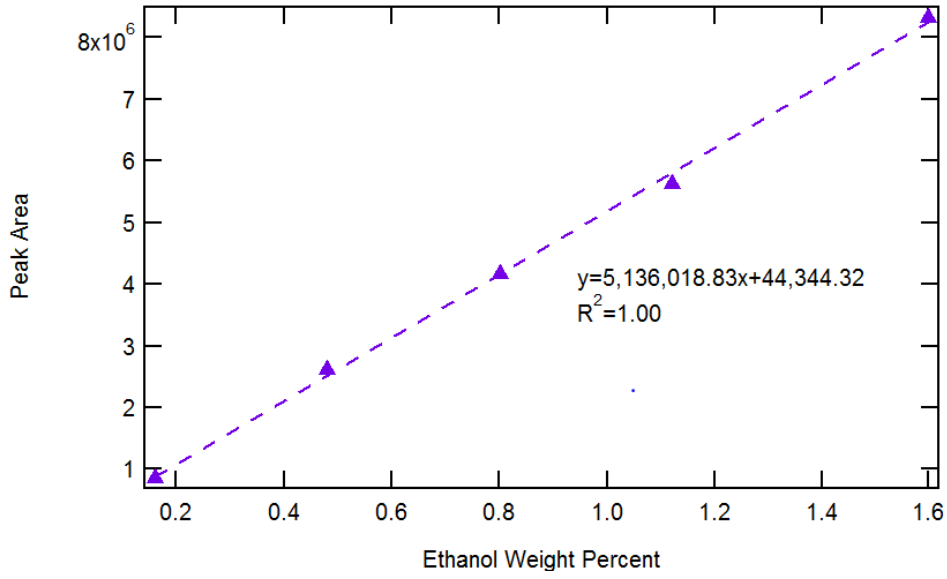

Figure 32: Ethanol Calibration Curve

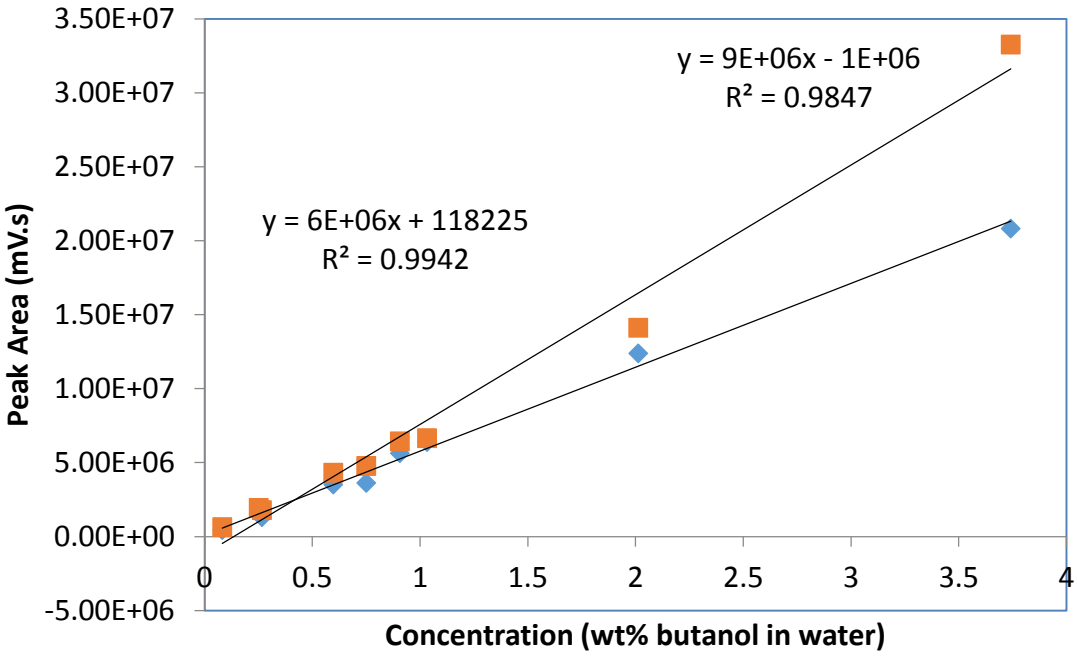

Figure 33: Butanol Calibration Curve

The butanol calibration curve was provided by another Worcester Polytechnic Institute project team studying butanol extraction. The butanol extraction team members are Allison Rivard, Chelsea Conlon, Mark Overdevest and David Knutson advised by Professor Thompsett.

Appendix D: Trial Parameters

Run Number	Phase	Temperature (°C)	Operating Pressure (PSI)	Catalyst Amount (g)	Ethanol Feed Flowrate (mL/min)	Water Feed Flowrate (mL/min)	Feed Ratio
1	Liquid	300	3600	0.5051	0.5	0	1.00
2	Liquid	300	3600	0.5003	0.3	0	1.00
3	Failed Trial- Slow Depressurization						
4	Liquid	300	3600	0.5263	0.5	0	1.00
5	Failed Trial						
6	Failed Trial						
7	Liquid	300	3300	0.5226	0.5	0	1.00
8	Liquid	250	3200	0.509	0.5	0	1.00
9	Liquid	300	3200	0.5023	0.5	0	1.00
10	Liquid	300	3200	1.02	0.5	0	1.00
11	Liquid	300	2800	1.001	0.5	0	1.00
12	Liquid	300	2700	0.62	0.5	0	1.00
13	Vapor	300	14.7	0.62	0.5	0	1.00
14	Vapor	300	14.7	0.62	0.5	0	1.00
15	Liquid	390	3600	0.3	0.5	0	1.00
16	Vapor	390	14.7	0.3	0.5	0	1.00
17	Vapor	345	14.7	0.3	0.5	0	1.00
18	Liquid	345	3500	0.3	0.5	0	1.00
19	Vapor	300	14.7	0.3	0.5	0	1.00
20	Liquid	390	3600	0.3	0.5	0.125	0.80
21	Liquid	420	3600	0.3	0.5	0.5	0.50
22	Vapor	390	14.7	1.6	0.05	0.025	0.66
23	Liquid	390	3600	0.02	1.5	0.75	0.66
24	Liquid	390	3600	0.02	0.75	0.375	0.66
25	Vapor	390	14.7	1.6	0.1	0.05	0.66
26	Liquid	390	3600	0.02	0.15	0.075	0.66
27	Vapor	390	14.7	1.6	0.5	0.25	0.66
28	Liquid	390	3600	0.02	0.3	0.15	0.66
29	Liquid	390	3600	0.02	1.5	0.75	0.66
30	Vapor	390	14.7	1.6	0.25	0.125	0.66
31	Liquid	390	3600	0.02	0.3	0.15	0.66
32	Liquid	390	3600	0.02	0.5	0.25	0.66
33	Liquid	390	3600	0.02	0.3	0.15	0.66
34	Vapor	390	14.7	1.6	0.05	0.025	0.66
35	Vapor	390	14.7	1.6	0.25	0.125	0.66
36	Vapor	390	14.7	1.6	0.35	0.18	0.66
37	Vapor	390	14.7	1.6	0.2	0.1	0.66
38	Vapor	390	14.7	1.6	0.15	0.77	0.66
39	Vapor	390	14.7	1.6	0.3	0.154	0.66
40	Liquid	390	3600	0.01	1.25	0.643	0.66
41	Liquid	390	3600	0.01	1.85	0.95	0.66

Figure 34: Complete Trial Parameters

Appendix E: In-Line GC-FID Intensity Graphs

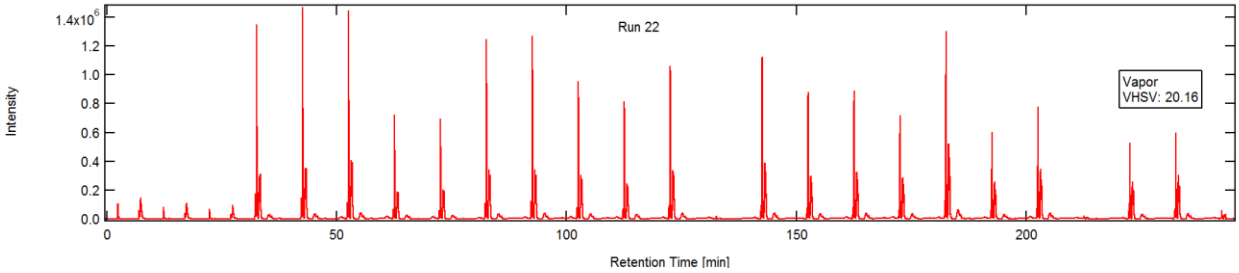

Figure 35: Run 22, Vapor Phase, VHSV: 20.16

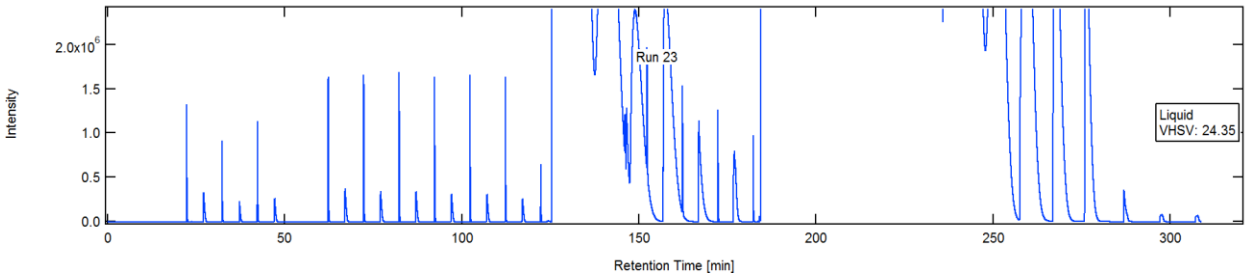

Figure 36: Run 23, Liquid Phase, VHSV: 24.35

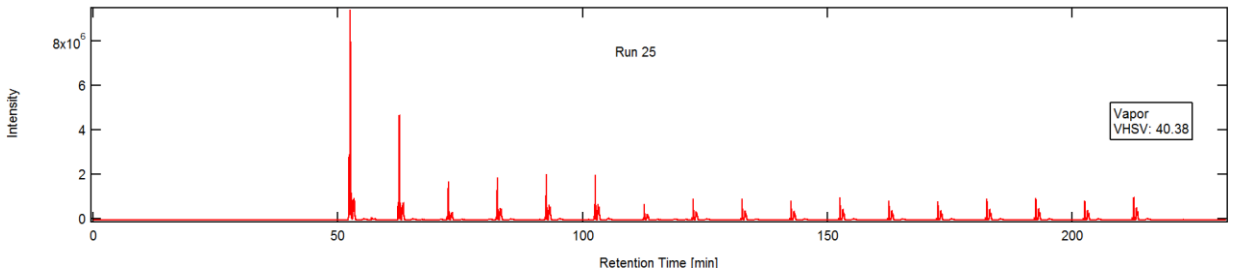

Figure 37: Run 25, Vapor Phase, VHSV: 40.38

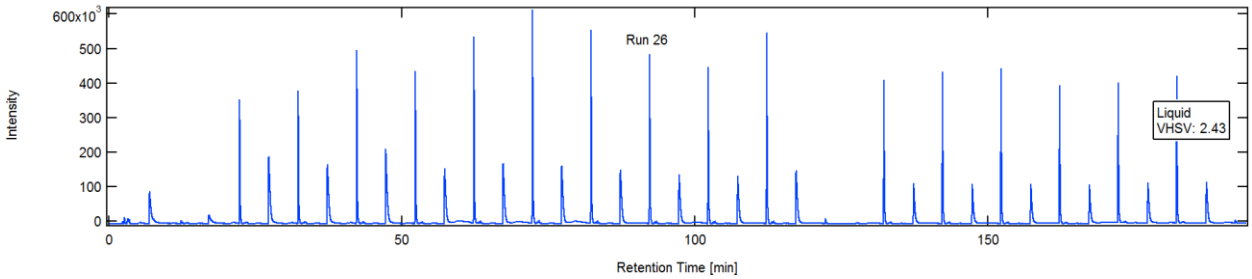

Figure 38: Run 26, Liquid Phase, VHSV: 2.43

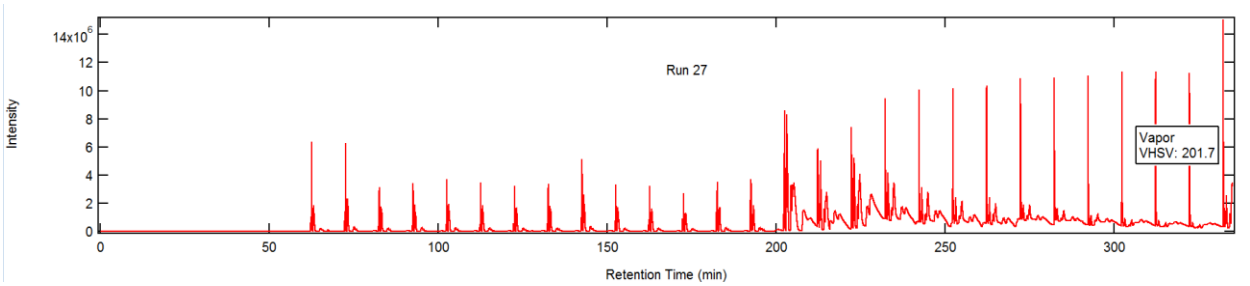

Figure 39: Run 27, Vapor Phase, VHSV: 201.7

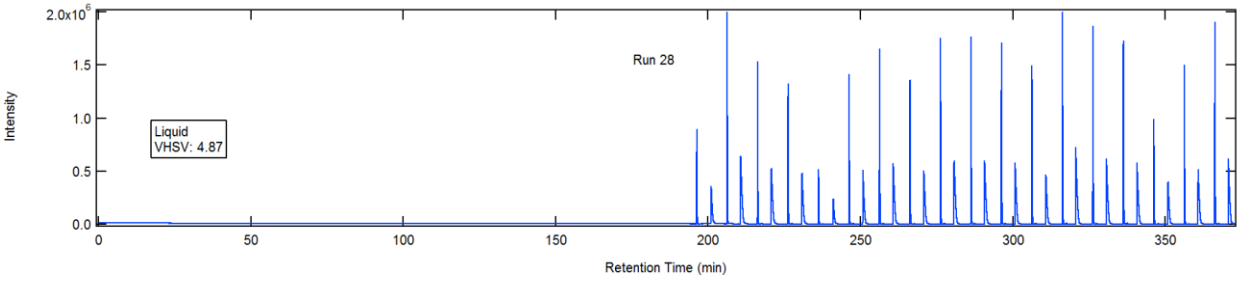

Figure 40: Run 28, Liquid Phase, VHSV: 4.87

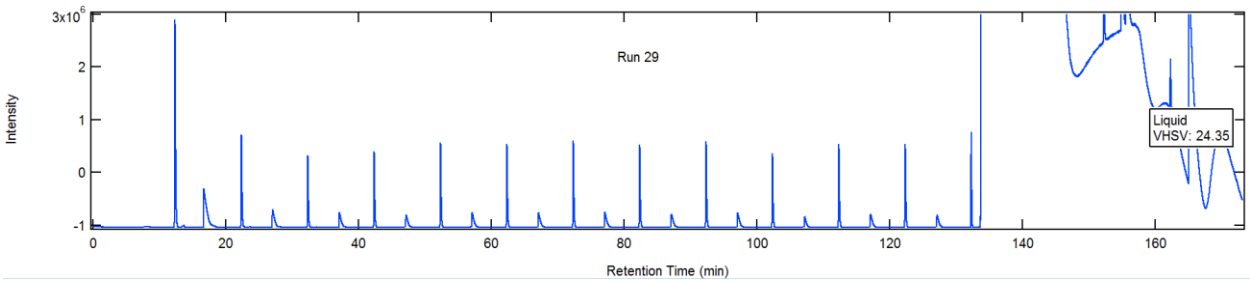

Figure 41: Run 29, Liquid Phase, VHSV: 24.35

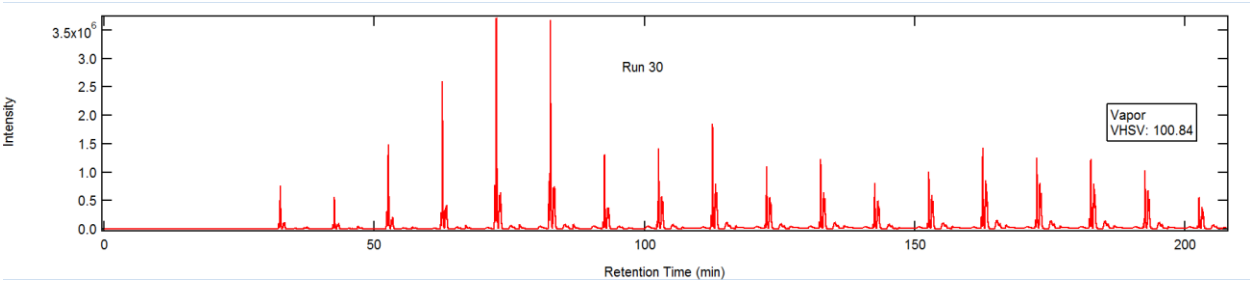

Figure 42: Run 30, Vapor Phase, VHSV: 100.84

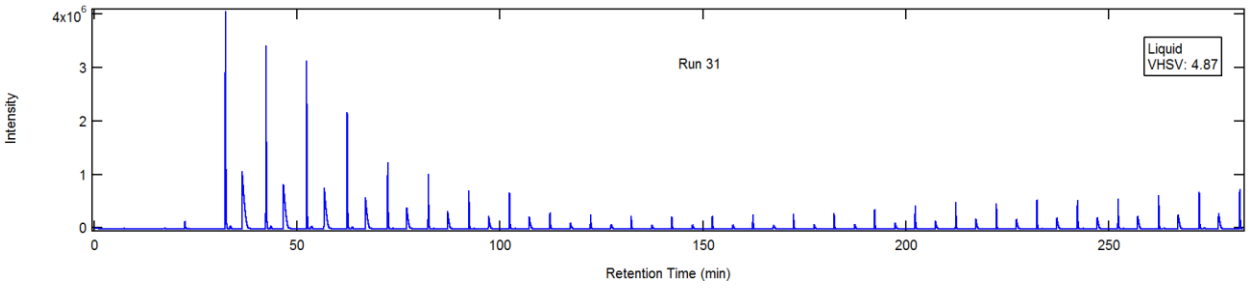

Figure 43: Run 31, Liquid Phase, VHSV: 4.87

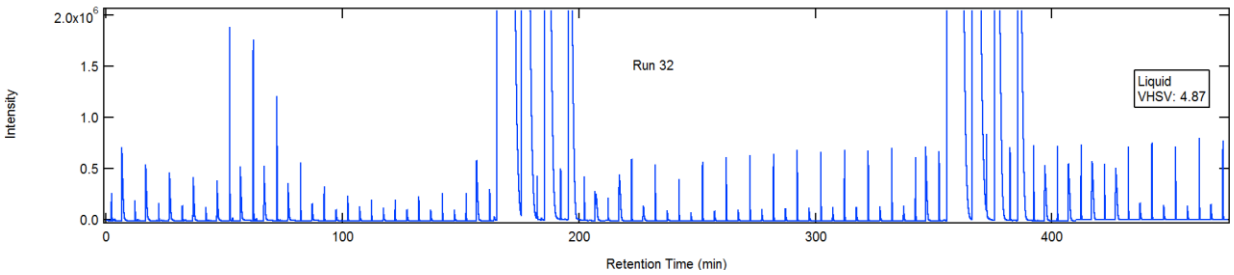

Figure 44: Run 32, Liquid Phase, VHSV: 4.87

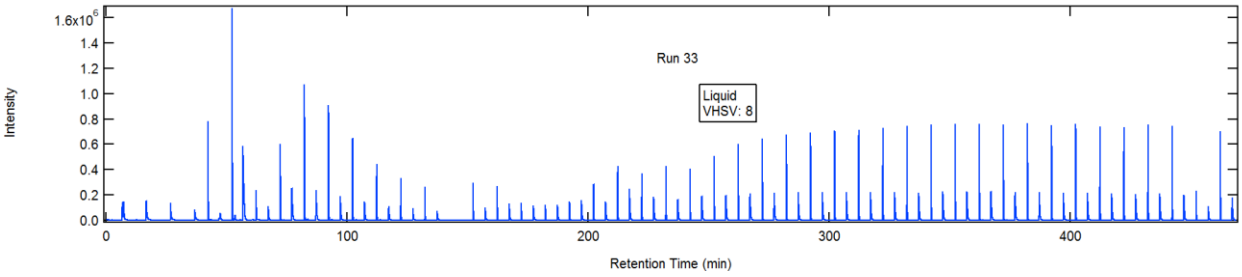

Figure 45: Run 33, Liquids Phase, VHSV: 8.12

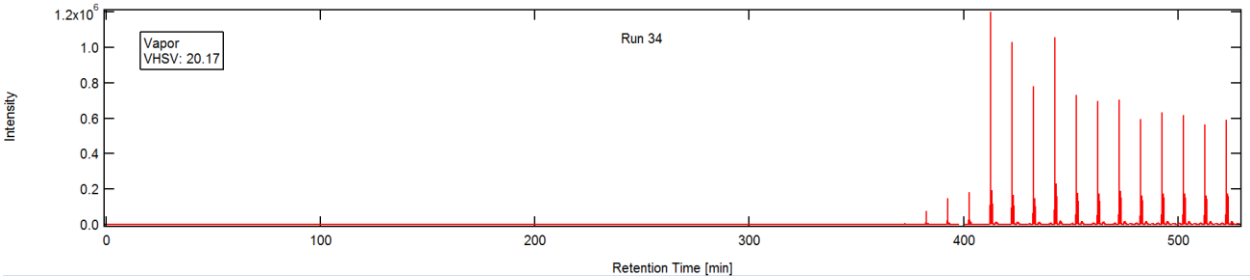

Figure 46: Run 34, Vapor Phase, VHSV: 20.17

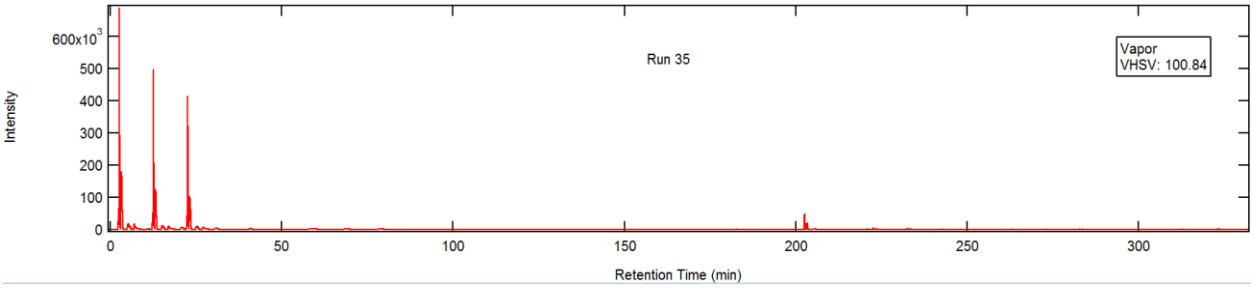

Figure 47: Run 35, Vapor Phase, VHSV: 100.84

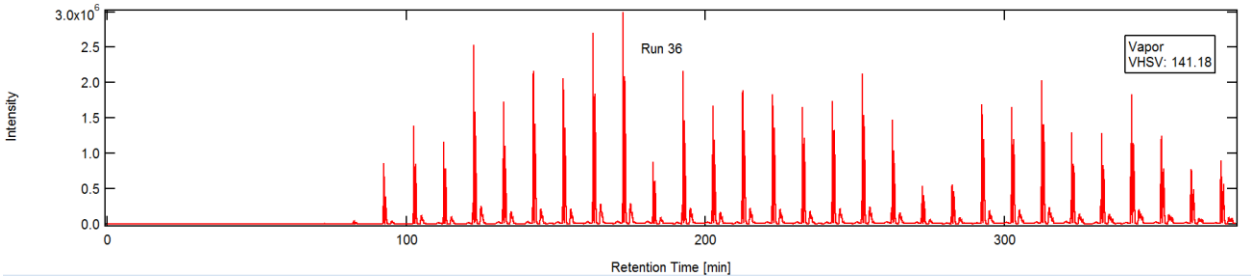

Figure 48: Run 36, Vapor Phase, VHSV: 141.18

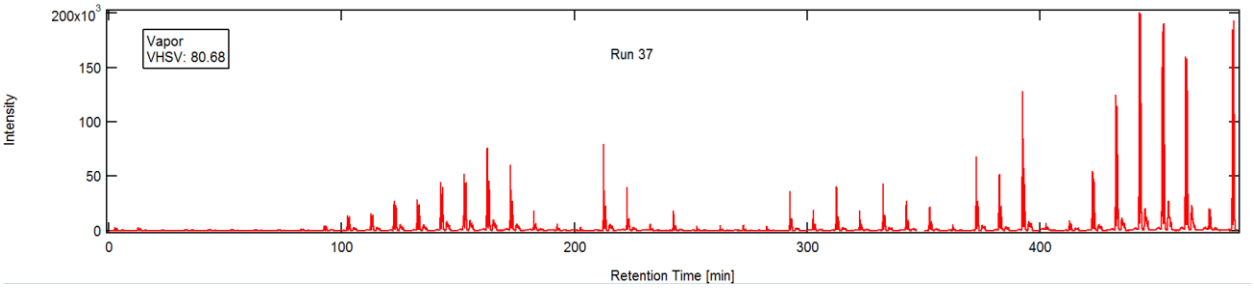

Figure 49: Run 37, Vapor Phase, VHSV: 80.68

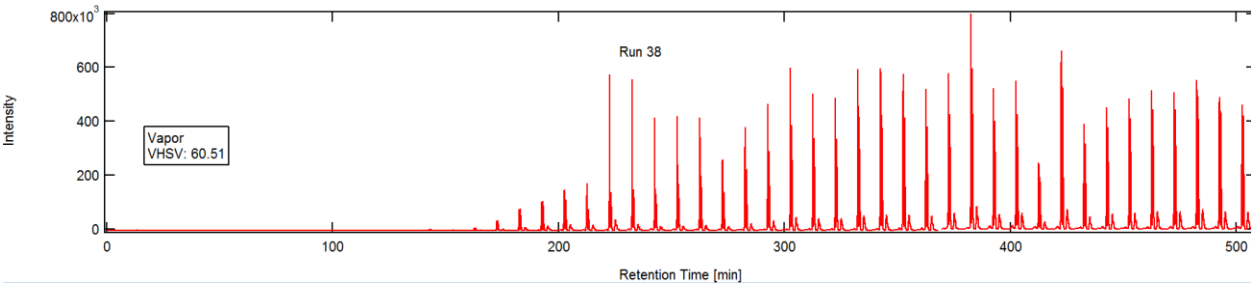

Figure 50: Run 38, Vapor Phase, VHSV: 60.51

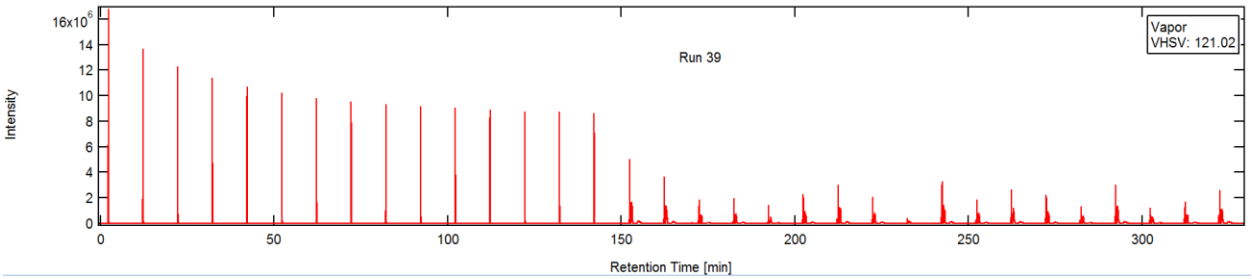

Figure 51: Run 39, Vapor Phase, VHSV: 121.02

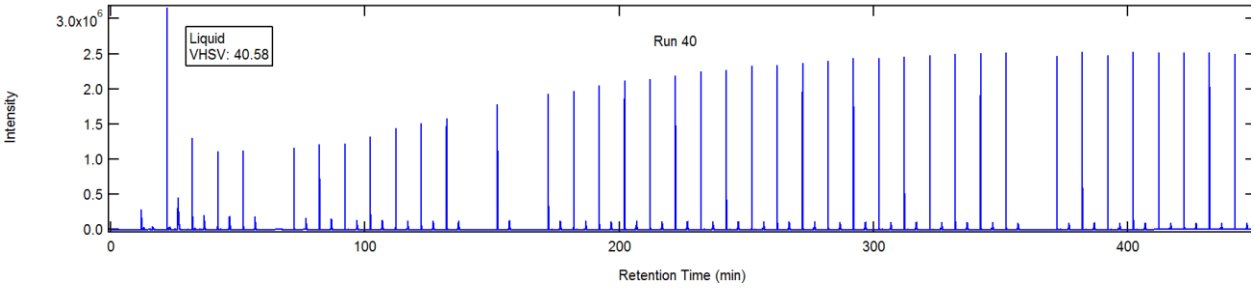

Figure 52: Run 40, Liquid Phase, VHSV: 40.58

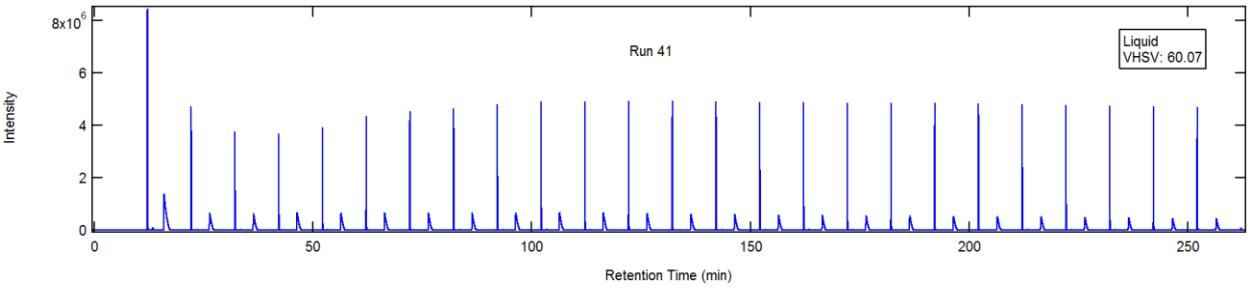

Figure 53: Run 41, Liquid Phase, VHSV: 60.07

Appendix F: Liquid Product Analysis Graphs

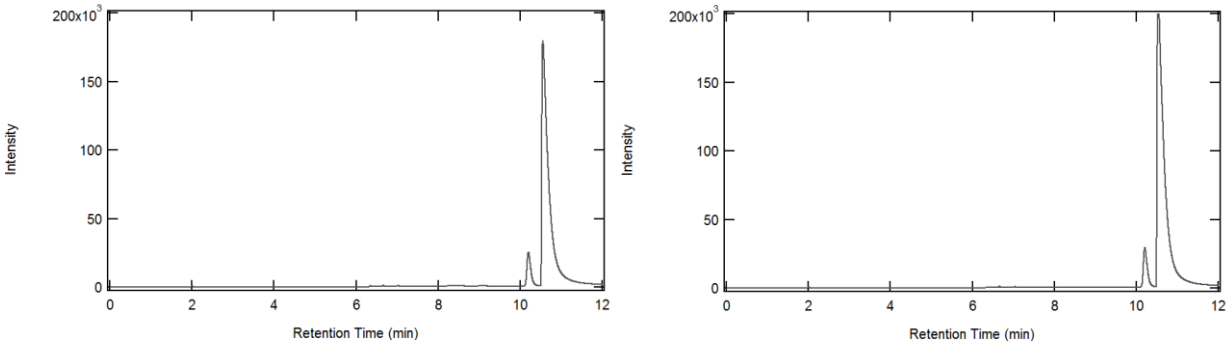

Figure 53: Liquid Phase, VHSV: 12.17

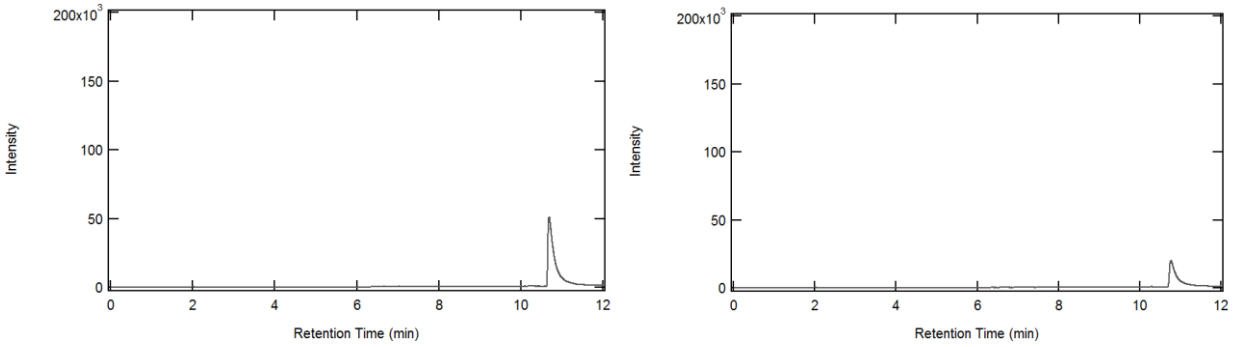

Figure 54: Vapor Phase, VHSV: 40.38

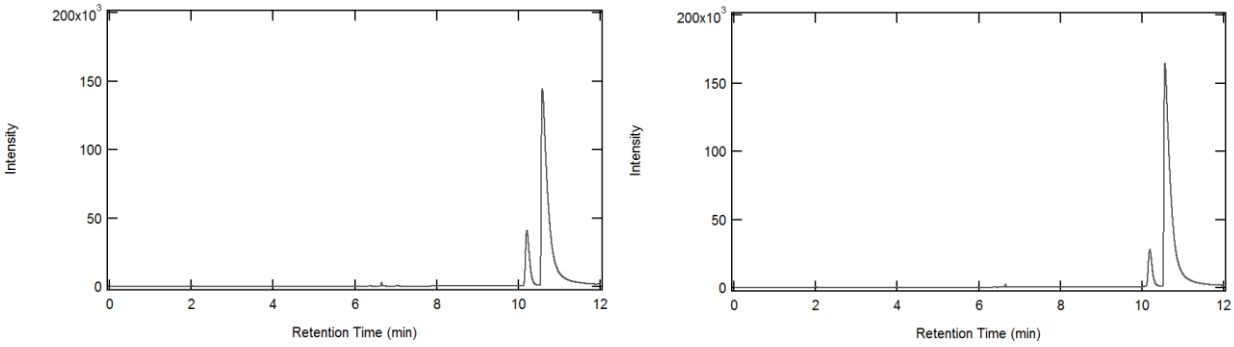

Figure 55: Liquid Phase, VHSV: 2.43

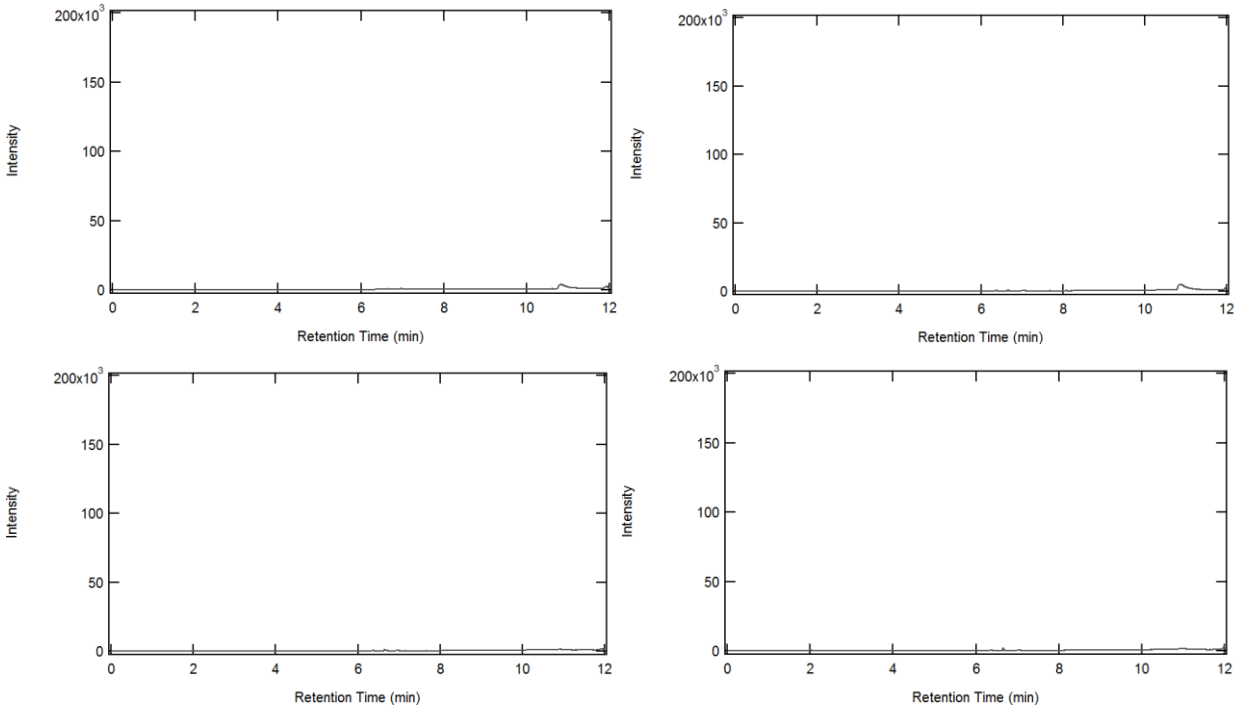

Figure 56: Vapor Phase, VHSV: 201.7

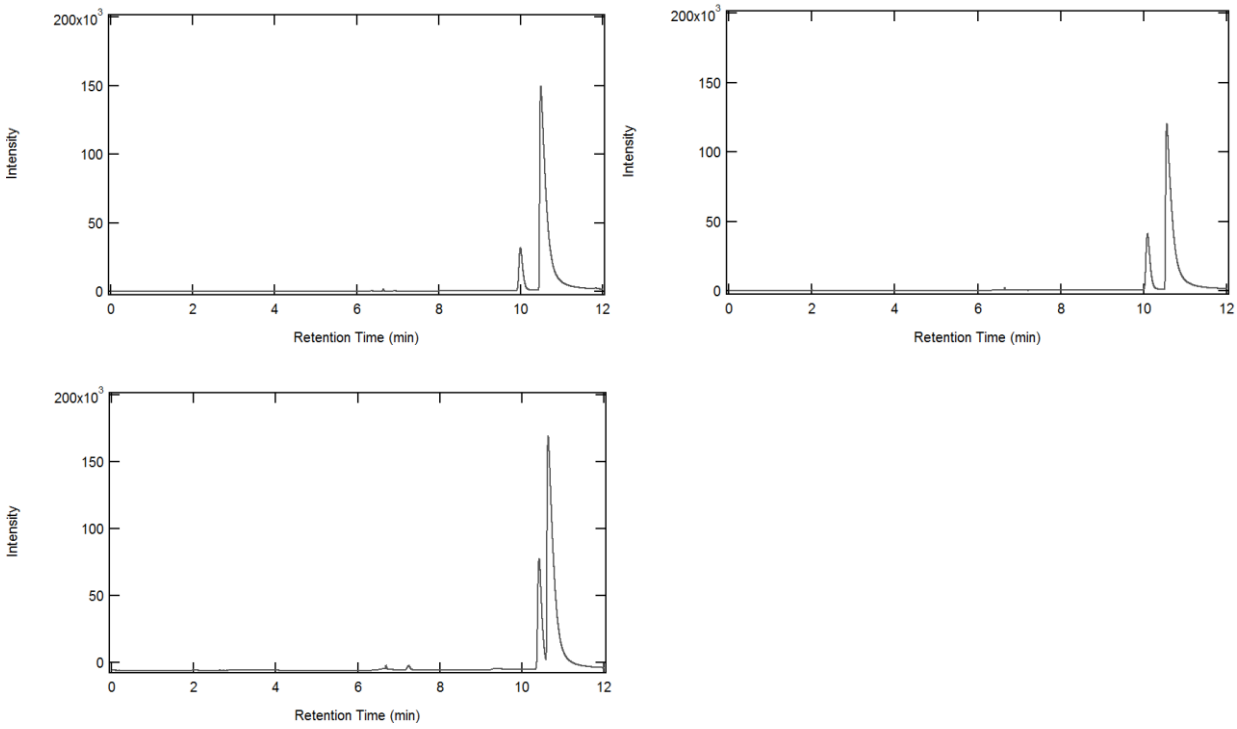

Figure 57: Liquid Phase, VHSV: 4.87

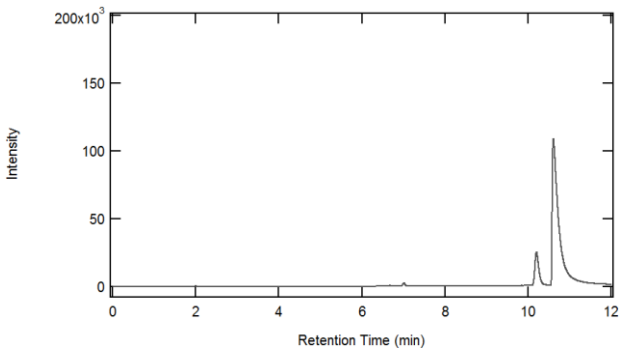

Figure 58: Liquid Phase, VHSV: 24.35

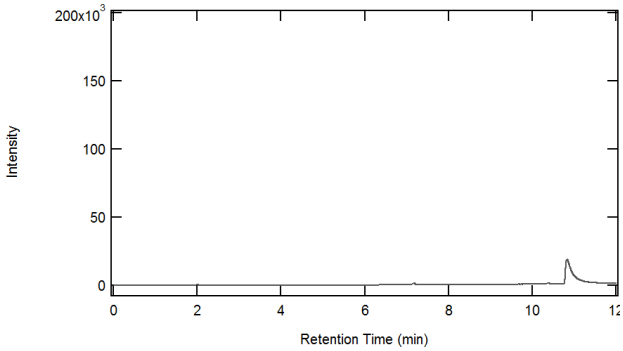

Figure 59: Vapor Phase, VHSV: 100.84

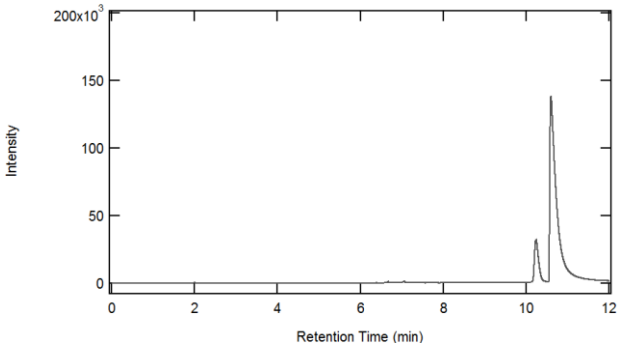

Figure 60: Liquid Phase, VHSV: 4.87

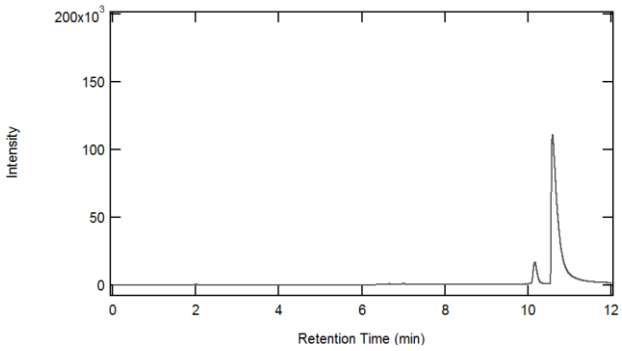

Figure 61: Liquid Phase, VHSV: 8

Appendix G: Raw Data

Vial #	Phase	VHSV	Peak Area	Vial wt%	EtOH wt%	EtOH mol%	Conversion
22.1	Vapor	20.16	7.63E+05	0.14	25.00	11.54	88.5
22.2	Vapor	20.16	3.33E+05	0.06	10.03	4.18	95.8
23.1	Liquid	24.35	2.54E+06	0.49	86.72	71.87	28.1
23.2	Liquid	24.35	2.53E+06	0.48	86.29	71.12	28.9
24.1	Liquid	12.17	2.65E+06	0.51	90.71	79.26	20.7
24.2	Liquid	12.17	2.26E+06	0.43	76.87	56.53	43.5
24.3a	Liquid	12.17	2.59E+06	0.50	88.67	75.38	24.6
24.3b	Liquid	12.17	1.99E+06	0.38	67.72	45.09	54.9
24.4	Liquid	12.17	2.49E+06	0.48	84.98	68.89	31.1
25.1	Vapor	40.38	5.40E+05	0.10	17.22	7.53	92.5
25.2	Vapor	40.38	1.91E+04	0.00	-0.88	-0.34	100.3
26.1	Liquid	2.43	1.62E+06	0.31	54.67	32.07	67.9
26.2	Liquid	2.43	1.83E+06	0.35	62.09	39.06	60.9
27.1	Vapor	201.69	3.68E+04	0.00	-0.26	-0.10	100.1
27.1b	Vapor	201.69	5.42E+04	0.00	0.34	0.13	99.9
27.2a	Vapor	201.69	0.00E+00	-0.01	-1.54	-0.60	100.6
27.2b	Vapor	201.69	0.00E+00	-0.01	-1.54	-0.60	100.6
28.1	Liquid	4.87	1.64E+06	0.31	55.63	32.92	67.1
28.2	Liquid	24.35	1.32E+06	0.25	44.47	23.86	76.1
28.3	Liquid		1.73E+06	0.33	58.62	35.66	64.3
29.1	Liquid	24.35	1.16E+06	0.22	38.80	19.87	80.1
30.1	Vapor	100.84	2.27E+05	0.04	6.33	2.58	97.4
32.1	Liquid	4.87	1.52E+06	0.29	51.47	29.33	70.7
33.1	Liquid	8	1.25E+06	0.24	42.08	22.14	77.9

Figure 62: Conversion Data Table

Run Number	Phase	VHSV	Nitrogen Flow	Area	uL Ethylene	mL ethylene	Vol % Ethylene	Vol % Nitrogen	Flowrate Ethylene (mL/min)	Flowrate Ethylene (g/min)	Flowrate Ethylene (mol/min)	Flowrate Ethanol (ml/min)	Flowrate Ethanol (g/min)	Flowrate Ethanol (mol/min)	Yield
34	Vapor	20.16	159.914712	478771.375	1.36096077	0.00136096	0.02268268	0.97731732	3.71148048	0.00668066	0.00023817	0.05	0.06337136	0.00137559	17.3139965
25	Vapor	40.38	149.253731	683138.125	1.40815625	0.00140816	0.02346927	0.97653073	3.58706196	0.00645671	0.00023019	0.1	0.12674271	0.00275118	8.36679307
38	Vapor	60.51	151.821862	515565.286	1.36945778	0.00136946	0.0228243	0.9771757	3.54616591	0.0063831	0.00022756	0.15	0.19011407	0.00412677	5.51426891
39	Vapor	121.02	160.25641	1525997	1.60280204	0.0016028	0.02671337	0.97328663	4.39848674	0.00791728	0.00028226	0.3	0.38022814	0.00825355	3.4198116
36	Vapor	141.18	155.440415	2162114.36	1.74970393	0.0017497	0.02916173	0.97083827	4.6690699	0.00840433	0.00029962	0.35	0.44359949	0.00962914	3.11159081
27	Vapor	201.69	147.275405	82850123.1	20.383406	0.02038341	0.33972343	0.66027657	75.7756804	0.13639622	0.00486261	0.5	0.63371356	0.01375592	35.3492325
26	Liquid	2.43	161.637931	3126582	1.97243347	0.00197243	0.03287389	0.96712611	5.49428631	0.00988972	0.00035257	0.15	0.19011407	0.00412677	8.54358563
33	Liquid	4.87	156.087	6655143.88	2.78730263	0.0027873	0.04645504	0.95354496	7.60428587	0.01368771	0.00048798	0.3	0.38022814	0.00825355	5.9123118
32	Liquid	8	163.755	6030427.75	2.64303369	0.00264303	0.04405056	0.95594944	7.54590086	0.01358262	0.00048423	0.5	0.63371356	0.01375592	3.52015056
24	Liquid	12.17	163.934426	9915719.36	3.54028431	0.00354028	0.05900474	0.94099526	10.2794438	0.018503	0.00065964	0.75	0.95057034	0.02063387	3.19689597
23	Liquid	24.35	163.934426	12181702.2	4.06357952	0.00406358	0.06772633	0.93227367	11.9092457	0.02143664	0.00076423	1.5	1.90114068	0.04126775	1.8518813
29	Liquid	24.35	158.730159	14121025.6	4.51143759	0.00451144	0.07519063	0.92480937	12.905384	0.02322969	0.00082815	1.5	1.90114068	0.04126775	2.00678026

Figure 63: Yield Data Table

Run Number	Phase	VHSV	Catalyst Mass (g)	Average Ethylene Peak Area	Nitrogen Flowrate (mL/min)	Etylene Peak Area Normalized for Nitrogen Flowrate	Average Ethylene Peak Area per Gram of Catalyst	Average Total Carbon Peak Area	Total Carbon Peak Area Normalized for Nitrogen Flowrate	Average Total Carbon Peak Area per Gram of Catalyst
26	Liquid	2.43	0.02	3.13E+06	161.64	1.93E+04	9.67E+05	-	-	-
33	Liquid	4.87	0.02	6.66E+06	156.09	4.26E+04	2.13E+06	-	-	-
32	Liquid	8	0.02	6.03E+06	163.76	3.68E+04	1.84E+06	-	-	-
24	Liquid	12.17	0.02	9.92E+06	163.93	6.05E+04	3.02E+06	-	-	-
23	Liquid	24.35	0.02	1.22E+07	163.93	7.43E+04	3.72E+06	-	-	-
29	Liquid	24.35	0.02	1.41E+07	158.73	8.90E+04	4.45E+06	-	-	-
40	Liquid	40.58	0.01	1.03E+07	160.26	6.43E+04	6.43E+06	-	-	-
41	Liquid	60.07	0.01	2.01E+07	158.39	1.27E+05	1.27E+07	-	-	-
34	Vapor	20.16	1.6	4.79E+05	159.91	2.99E+03	1.87E+03	9.54E+06	5.97E+04	3.73E+04
25	Vapor	40.38	1.6	6.83E+05	149.25	4.58E+03	2.86E+03	1.49E+07	9.98E+04	6.24E+04
36	Vapor	60.51	1.6	5.16E+05	151.82	3.40E+03	2.12E+03	1.47E+07	9.70E+04	6.06E+04
27	Vapor	121.02	1.6	1.32E+06	160.26	8.25E+03	5.16E+03	2.47E+07	1.54E+05	9.63E+04
36	Vapor	141.18	1.6	2.16E+06	155.44	1.39E+04	8.69E+03	4.57E+07	3.05E+05	1.90E+05
27	Vapor	201.69	1.6	8.29E+07	147.28	5.63E+05	3.52E+05	9.55E+07	6.49E+05	4.05E+05

Figure 64: Throughput Data Table

Appendix H: Poster

Ethanol Dehydration with ZSM-5

Jennifer Coffey (ChE), Alexander Zitoli (ChE)
Advisor: Professor Michael Timko (Chemical Engineering)

Abstract

This project studied ethanol dehydration with ZSM-5 to explore the benefits of liquid phase versus vapor phase dehydration. In collaboration with a PhD candidate, the project team of two WPI seniors conducted background research and extensive experimental trials.. The process variables manipulated were phase, feed flow rate ratios, and volume-hourly space velocity. Through gas chromatography, mass spectroscopy, and graphical analysis, the project team determined that liquid phase dehydration had comparable ethanol conversion, superior ethylene yield, and throughput when compared to the vapor phase. The team recommends further optimization of the process variables for liquid phase dehydration.

1 The Growing Importance of Bio-plastics

- Industrial leaders, like Braskem, have had success with gas phase catalytic dehydration of bio-ethanol to create "green ethylene".[2]
- Various catalysis studies have shown that ZSM-5 as a catalyst for the dehydration of ethanol yields the highest combination of selectivity and efficiency.[3] Liquid phase dehydration could yield lower energy costs.

Challenges for Ethanol Dehydration

- Bio-ethanol from fermentation broth requires drying.
- Ethanol feedstock is localized to crop centers, costly transport.
- Zeolite stability aqueous conditions.
- Catalyst coking requiring industrial regeneration.
- Vapor phase requires extra separation steps.

2 Experimental

- Continuous flow reaction through packed-bed reactor

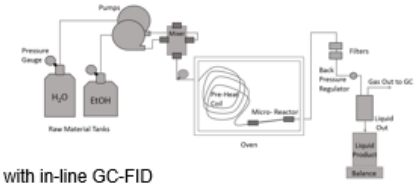

- Analysis with in-line GC-FID

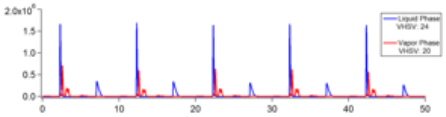

- Systematic study of: Liquid VHSV, Vapor VHSV, Feed Ratio
- Comparison weight-hourly space velocity and volume-hourly space velocity

3 Orders of Magnitude Difference

$$WHSV = \frac{\dot{m}_{EtOH}}{\text{mass catalyst}} \qquad VHSV = \frac{\dot{V}_{EtOH}}{\text{volume catalyst}}$$

3 Results

Overlay of GC-FID Raw Data

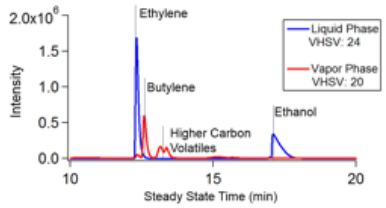

- Liquid phase showed much greater ethylene production, with less ethanol conversion and fewer additional products.
- Vapor phase dehydration show low ethylene production, increased production of additional products and better conversion.

VHSV Comparison

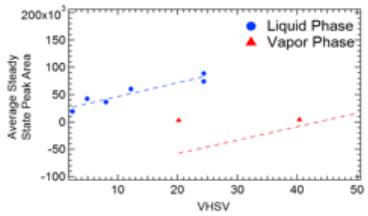

- When comparing peak area at each VHSV, liquid phase dehydration shows a slight advantage

Throughput Comparison

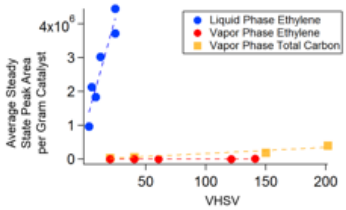

- On a per gram of catalyst basis, liquid phase ethanol dehydration shows a significant advantage.
- At low VHSVs, vapor phase ethanol dehydratior produces substantially less carbon products.

4 Conclusion: A Liquid Phase Advantage

- Liquid phase ethanol dehydration generates more ethylene at higher throughput- increasing industrial efficiency.
- Ethanol dehydration in the liquid phase also works very well with a feed that is not pure ethanol. This can reduce industrial drying needs.
- Vapor phase ethanol dehydration can produce high value products at very low volume hourly space velocity.
- Further testing and optimization of the ethanol dehydration process is needed before industrial scale-up.

Acknowledgements

The project team thanks Professor Michael Timko, our advisor, for his constant encouragement and ability to engage us in this project. His vision for the success of the project inspired us to work beyond expectations. Additionally, we would like to thank Alex Maag, a chemical engineering PhD Candidate, for the countless hours of assistance inside the laboratory and for the support with research and data analysis outside of the laboratory.

References

1. Luiz, Paulo, Augusto Monte, Luiz F. Cassinelli, Antonio Morschbacker, and Roberto Wermeck Do Carmo. "Braskem's Ethanol to Polyethylene Process Development." *Catalytic Process Development for Renewable Materials* 1 (2012): 149-65. Web.
2. Zhang, Xian, Rijie Wang, Xiaoxia Yang, and Fengbao Zhang. "Comparison of Four Catalysts in the Catalytic Dehydration of Ethanol to Ethylene." *Microporous and Mesoporous Materials* 116.1-3 (2008): 210-15. *Science Direct*. Web. 26 Sept. 2015. <http://www.sciencedirect.com/science/article/pii/S1387181108001819>.